NASA Contractor Report 4488

Advanced Reinforcement Systems for Intermetallic Applications

Howard F. Merrick and Mohammed L. Labib

CONTRACT NAS3-25970
MARCH 1993

NASA

NASA Contractor Report 4488

Advanced Reinforcement Systems for Intermetallic Applications

Howard F. Merrick and Mohammed L. Labib
Textron Lycoming
Stratford, Connecticut

Prepared for
Lewis Research Center
under Contract NAS3-25970

National Aeronautics and
Space Administration

Office of Management

Scientific and Technical
Information Program

1993

ADVANCED REINFORCEMENT SYSTEMS FOR INTERMETALLIC APPLICATIONS

H.F. Merrick
Textron Lycoming
Stratford, Connecticut 06497-7593

and

M.L. Labib
David Sarnoff Research Center
SRI International
CN5300
Princeton, New Jersey 08543-5300

ABSTRACT

A 2-D axisymmetric model was employed to determine the magnitude of the radial, axial and hoop stresses caused by the thermal expansion difference between fiber and matrix and which result from the fabrication temperature cycle. Finite element analysis was conducted for single fiber model systems based on SCS-6/Ti_3Al+Nb and Al_2O_3/NiAl. The stress distribution due to the imposition of a graded intermediate layer for each system was determined and included variables of layer thickness and gradation in interlayer chemistry in order to vary the expansion gradient between fiber and matrix.

Thermal cycling tests were conducted on sputter coated SCS-6 fibers selectively coated with Ti_3Al+Nb with and without an intermediate layer. Cracking of the Ti_3Al+Nb layers was prevented by an interlayer based on Ti-TiN-Ti. The interlayer thickness appeared critical to its efficacy. Similarly, for the case of Al_2O_3/NiAl, an intermediate layer consiting of a Ni bond coat on the sapphire fiber followed by a graded Al_2O_3-NiAl layer did not crack when given a thermal excursion to 1100°C and then cooled to room temperature.

Acoustic emission tests on single fiber specimens were unsuccessful in detecting load drops associated with the successive fracture of the fiber. For the SCS-6/Ti_3Al system this was the result of several factors which included the matrix/fiber ratio and poor bonding of the matrix and fiber. In the case of the Al_2O_3/NiAl system brittle failure of the NiAl matrix precluded fiber breakdown during tensile loading.

I. INTRODUCTION

Advanced gas turbine engines require next generation materials that can be used under severe temperatures and mechanical stresses. These demanding requirements limit the choice of materials to very few candidates. Fiber-reinforced composites based on intermetallics are candidates for such applications because of their low densities and high temperature capabilities. However, several fundamental problems must be solved for the successful application of these materials.

The fiber and matrix must retain useful mechanical properties at high temperatures, and must possess chemical and thermal compatibility between the fiber and matrix. Fiber reaction with the matrix at high temperatures often leads to the formation of an interfacial reaction zone, which can cause deterioration in the mechanical strength of the composite. Thermal expansion mismatch between the fiber and matrix may result in matrix cracking in the interface region that can result in loss of properties.

All of these critical problems involved processes occurring in the interfacial region between the fiber and matrix. Evaluation of what takes place in this region and of ways to modify its properties is key to the development of improved composites. Since the choice of fibers is very limited, the use of fiber coatings is an attractive means to control the properties of the interfacial region. A fundamental understanding of the nature and magnitude of interface stress is required to develop effective solutions to the above problems.

The objective of this research was to evaluate the feasibility and effectiveness of graded composition intermediate layers (between fiber and matrix) in minimizing stress due to thermal expansion mismatch between the fiber and matrix. Two intermetallic matrix composites, SCS-6/Ti_3Al+Nb and Al_2O_3/NiAl, were selected for this study;

- A graded layer based on Ti-TiN-Ti composition was selected for the SCS-6/Ti_3Al+Nb composite,

- A graded layer based on Ni/Al/Al_2O_3/Ni/Al was selected for Al_2O_3/NiAl composite. This material combination gives a gradual transition between $A1_2O_3$ and NiAl properties.

The program was divided into two major tasks and contained both Finite Element Modeling (FEM) analysis and experimental investigations. Task I evaluated the thermal stresses of uncoated fiber-matrix systems. The magnitude of thermal stress was measured and correlated with results of the FEM analysis. The purpose of the Task I results was to identify trends, develop confidence in the analytical methodology and establish baseline criteria for selecting materials, conditions and parameters in Task II. In Task II, the effectiveness of intermediate layers having graded compositions was investigated. Specifically, the objectives were to design intermediate layers with the guidance of FEM analysis. The intermediate layer would have a gradual increase in thermal expansion coefficient past the fiber surface. The layer would be ceramic-like near the fiber and approach the composition of the pure metal at the matrix interface. Interfacial thermal stresses and chemical properties were characterized.

It was the intent of the program to develop intermediate coating layers consisting of reaction barrier and thermal expansion coefficient matching layers in order to scale-up engineering for composite production in future years.

II. PROCEDURES

A. SINGLE FIBER MODEL

A 2-D axisymmetric model was used to simulate a unit cell composite consisting of three concentric cylinders representing the fiber, interfacial layer, and matrix, respectively. Figure 1 shows the FEM model with a detailed description of the boundary conditions applied in this study. The FEM model contains a fine mesh in the fiber-matrix interface for accurate analysis results. The effective material properties of the interfacial layer (Ref. 1,2) were approximated from the basic properties of the fiber and the matrix using the property gradation formula given in Figure 2 as suggested by Dr. S. Arnold of NASA-Lewis Research Center. The FEM analysis was performed using the ANSYS program on the Cyber 910/920 system. The FEM models included the following features:

1. 2-D axisymmetric elements with central symmetry plane at y = 0.0 (Figure 1-a).

2. NASA suggested boundary conditions (Figure 1-b)

   a. Single fiber composite of infinite length,

   b. Generalized plane strain at the top end surface (y = 0.5),

   c. Free cylindrical surface.

3. Both elastic and elastic-plastic modeling were investigated in Task I.

   The FEM model was verified using an analytical solution for a simple composite system (single fiber composite without interfacial layer).

B. RESIDUAL STRESSES

Flat substrates were employed to evaluate the residual thermal stress and the nature of cracking in the matrix layer when coated with thin films.

In these experiments, both NiAl and Ti_3Al+Nb were deposited onto single crystal sapphire wafers by sputtering. A suitable SiC wafer for depositing Ti_3Al+Nb could not be obtained. The thickness of films used was between 1.0 and 3.0 μm. The radius of curvature of annealed sapphire wafers, before and after depositing the matrix film, and wafers with the deposited matrix film subjected to temperature exposure were measured using the x-ray technique.

C. GRADED LAYERS

To develop the graded-CTE interface multilayer stack, we followed two parallel paths. First, we experimentally investigated a variety of graded-CTE multilayer stacks on flat substrates made of the fiber material. In these experiments thick layers of the matrix material were deposited on top of the multilayer stacks to simulate the fiber-graded layer-matrix combination. The resulting structures were then thermally cycled and examined to determine the effectiveness of the stack towards reducing cracking.

Second, the most successful layer combinations on flat substrates were deposited onto Al_2O_3 and SiC fibers followed by the deposition of thick layers of the matrix. These coated fibers were subsequently thermally cycled.

The Sarnoff multi-target reel-to-reel system fiber coating was used for depositing the coatings. The deposition sources are high-rate cylindrical magnetrons designed and constructed at Sarnoff. These magnetrons can be operated in a DC or RF mode, and permit the deposition of a variety of thin-film materials by DC/RF or reactive sputtering.

Improved cylindrical magnetrons with larger diameter targets, designed to lower the plasma bombardment of the fiber, were used. The reel-to-reel operation is computer controlled and permits uniform coatings to be deposited on long fiber lengths. This automatic control of fiber speed and rewind permits coating fibers with thin layers of different compositions and is critical for developing an effective graded-CTE stack.

D. ACOUSTIC EMISSION TEST SPECIMENS AND TEST PROCEDURE

Four Alpha-2 titanium aluminide plates (nominally Ti-24a/o Nb - 11 a/o Al) were machined from as forged stock. Each plate measured 88.9 x 50.8 x 7.6 mm. Two plates contained grooves so that each could receive three SCS-6 silicon carbide fibers, the depth of the grooves being about sixty percent of the fiber diameter. The mating plates contained no grooves. All plates were acid etched to provide clean mating surfaces.

Each pair of plates plus fibers, sealed by EB welding at the periphery were HIP bonded at 996°C for three hours at 103 MPa pressure. X-radiography was used to check fiber alignment. The ends of the plates were ground back to expose the fiber ends which then served as the center of axis for the test specimens. This procedure was used for both uncoated and coated fibers.

The $NiAl/Al_2O_3$ specimens were also machined from HIP bonded material. In this case a single sapphire fiber was suspended centrally in a mild steel tube of about 12.7 mm ID and -100/+325 mesh NiAl powder distributed about it, taking care to maintain fiber alignment. The tube was then sealed and HIP'ed at 1260°C for four hours and 138 MPa pressure. In several instances sealing was imperfect and

resulted in contamination of the NiAl during HIP. These samples were not used for preparing acoustic emission test specimens.

The acoustic emission test specimens were 76.2 mm inches long with a gauge length of 15.7 mm and gauge diameter of 4.9 mm. The ends of the specimens were machined flat. A 2273 kgm ATS screw-driven tensile machine was fitted with "45°" grips to mate with the shoulders of the test specimens.

The acoustic emission system was able to simultaneously measure and capture the following information: stress, strain, RMS acoustic emission events, arrival times to the top and bottom transducers located at the end of the specimen, and wave forms of "flagged" acoustic emission events.

The underlying principles of the techniques and equations used to calculate the critical fiber length are given in the paper by Clough et al, (Reference 4).

The fiber strength of a metallic matrix composite system was estimated using the magnitude of a load drop measured on the "hard" tensile testing machine that applies the acoustic emission technique to sense fiber fractures. It is given as:

$$\sigma_f = \Delta P(A_s/A_f)\ (d\sigma/d\epsilon)/(Kl_c) \qquad (1)$$

where

ΔP: load drop

A_s/A_f: ratio of cross-sectional area of test specimen and fiber

$d\sigma/d\epsilon$: work hardening rate

K: machine stiffness

l_c: critical length of fiber

Based on the fiber loading theory, the critical length for fiber fracture is expressed as:

$$l_c = \sigma_f d/(2\tau) \qquad (2)$$

where τ is the interfacial shear strength and d the fiber diameter. The critical fiber length is determined from the acoustic "events" and is verified by isolating the fragmented fibers by acid dissolution of the matrix.

RESULTS AND DISCUSSION

I. THERMAL STRESSES IN MODEL COMPOSITES

A. FEM ANALYSIS

Two fiber and matrix systems (Table 1) were investigated in this analysis. The first system comprised Al_2O_3 (F1) and NiAl (M1) and was designated case TSK13. The second system comprised SiC(F2), and Ti_3Al+Nb (M2), and also included an intermediate Ti-TiN-Ti layer. These cases were designated as TSK12, 14, 15 and 16. Both linear (elastic) and non-linear (inelastic) properties (Tables 2 and 3) were used in each case for comparison with the actual material behaviors. In the elastic cases, the yield strengths were used as failure criteria, while in the inelastic cases, both yield and ultimate strengths were used for the best failure judgment.

SCS-6/Ti_3Al+Nb System

The computer calculated stress values for both elastic and inelastic treatments are tabulated in Table 4.

For the case of TSK12 (thin Ti_3Al+Nb matrix layer on SCS-6 fiber) using elastic modeling, it was found that both the stress values and the stress states from the FEM analysis matched closely the analytical solutions determined by Arnold et al (3). Therefore, the 2-D FEM model was verified and proven to be sufficiently accurate. Consequently it was used in all subsequent analyses.

However, elastic modeling is not appropriate for this system. The calculated stresses were found to be greater than the yield strength either in the matrix layer or in the intermediate layers if the elastic model is applied. As a result elastic modeling will give over-estimated stress values since the material is already plastically deformed. Therefore, elastic-plastic modeling was adopted.

In this case, the FEM elastic-plastic stress analyses predicted that there would be no failure in different material layers since the calculated stress values were less than the ultimate strengths of the material. The axial stress had a steeply rising slope toward the outer radial locations in the matrix. The hoop stress, on the other hand, had a declining trend toward the outer radial locations in the matrix. The calculated stress levels were well below the yield strengths in the fiber and the graded layers. Therefore, only the elastic material properties for these layers were needed for performing the analyses.

No improvement was predicted when intermediate layers were introduced as a comparison of TSK15 (thin matrix with intermediate layer) with TSK12 shows. Neither a lowering of the axial stress values nor a shifting of high axial stresses from the interfacial region to the outer boundary of the matrix is likely to occur. The axial stress levels at the corresponding locations are predicted to increase by 25 percent to 35 percent when the intermediate layers are introduced while the hoop

stress is predicted to increase by 9 percent and 31 percent at the inner and the outer matrix surface, respectively. The rising slope of the axial stress is predicted to steepen, while the declining slope of the hoop stress is smoother.

For the case of a composite with intermediate layers, thick matrix and a lower fiber volume fraction (TSK16), the stress levels are predicted to increase significantly in the fiber; however, the stress values are lower than the material yield strengths. Therefore, the FEM analysis using elastic material properties for the fiber is still valid. Both the axial and the hoop stress levels at the relevant locations were predicted to be dramatically lower in the matrix in TSK16. For instance, when compared with TSK12, the axial stress was reduced by 33 percent at the outer matrix boundary and 87 percent, the inner boundary. The hoop stress is 26 percent lower at the inner matrix boundary and 70 percent lower in the outer boundary.

A comparison of TSK16 with TSK15 and TSK12 predicts that a composite with a thick matrix and lower fiber volume fraction has less chance to suffer material failure at the interfacial region (either at the fiber-matrix or intermediate layer-matrix interface boundary).

Al_2O_3/NiAl System

For the Al_2O_3/NiAl composite (no intermediate layer) the stress levels are predicted to be higher than for the case of SCS-6/Ti_3Al+Nb composite. Although the hoop does not exceed the yield strength of NiAl, the axial stress does. Since NiAl is brittle at room temperature it is likely that interfacial cracks can occur.

B. FABRICATION OF MODEL COMPOSITE AND EVALUATION OF THERMAL STRESSES

Flat Substrates

As a first step, sputtering trials were made in order to optimize the conditions for depositing the required matrix film chemical composition. The results of these experiments are shown in Table 5 and demonstrate that close control of the film chemistry could be readily achieved.

The radius of curvature of two annealed sapphire wafers, before and after depositing the matrix film, and with deposited matrix film after temperature exposure are shown in Figures 3 and 4. The deformation (δ) and stress in a film deposited on a circular single crystal substrate of radius r, may be estimated by

$$\delta = \frac{r^2}{2R}$$

$$\sigma = \frac{E\delta t_f^2}{3(1-\nu)r^2 t_f}$$

where: R is the radius of curvature

t_f is the thickness of the deposited film

T_s is the thickness of the substrate

E is the elastic modules of substrate

υ is the Poisson ration of the substrate

Table 6 summarizes the thermal stress data for the two cases examined, NiAl/sapphire and Ti_3Al+Nb/sapphire and represent the stress left in the structure after cooling to room temperature.

SEM examination of the matrix films of the two composite systems, showed that they cracked during the thermal exposure cycle, Figures 5 and 6. The residual stresses thus measured represent stresses remaining after matrix cracking and not the maximum stress experienced during the thermal exposure cycle.

The results of Table 6 indicate that the as-sputtered NiAl matrix does not result in stresses before the thermal cycle. The substrate radius before thermal exposure is >100 meters. The stress is developed after the thermal exposure cycle. The stress values tabulated represent the residual stress after some "relief" as the composite was cooled to room temperature. A change in the composition of the matrix film was noticed after the consolidation cycle, as well as an elemental segregation of Ni and Al. This result may indicate that the composition of the matrix at and near the interface may change during consolidation and actual application of the composite.

The Ti_3Al+Nb/Sapphire system shows residual stress in the as sputtered film before thermal exposure (Table 6, Sample #6). Residual stress of the system after thermal exposure is about 234 to 262 MPa. This stress is what remains after the development of cracks in the matrix film, as shown Figure 6. Again, the composition of the near interface matrix layer changes after the consolidation cycle.

C. INTERFACE SHEAR STRENGTH FOR UNCOATED FIBER SYSTEMS

1. SCS-6/Ti_3Al+Nb

Two critical parameters are required to determine interfacial shear strength and fiber strength inside the matrix. They are load drops associated with fiber failure and the critical length of fiber segments found in the specimens after testing. The theory predicts that in the case of uniform fiber-matrix bonding in slow tension the fiber would eventually fracture into equal critical segments. The critical length is used to compute the interfacial shear strength. Premature failure of the specimen before the manifestation of this equilibrium state would not produce satisfactory results.

The acoustic emission test was conducted on three single fiber specimens. Figure 7 shows the RMS acoustic emission results as a function of time for specimen AJ2. The critical length was calculated from the arrival times of the sound waves of each flagged events to each of the transducer. The results are given in Table 7. The sum of the broken fiber segments determined by the time of arrival was accurate within five percent of the actual length in two of the specimens. Twenty percent deviation was found in the third specimens which after acid etching the specimens, was found to contain a bent fiber. Table 8 presents the acid etching results of the three specimens used in the study. Only the long portion of the broken specimens was used in this experiment. We believe that the acoustic emission results produce more reliable data regarding fiber fracture. The microscopic examination of acid etched segments and their recovery from the acid bath is a tedious procedure as well.

In the case of AJ2 specimen, there was some change in the stress level which was thought to be associated with fiber fracture. The magnitude of drops was found to give unrealistic fiber strength and interfacial shear strength. The drop in stress was then discounted in our calculations. With the specimen dimensions used in the above measurements and assuming that the fiber strength stays at the 100 percent level, the load drop detected would be about 0.05 kgm. This is even below the detection limit of the load cell, which is 0.05 kgm.

The above results are similar to Clough's measurements in the case of the slowly grown matrix single aluminum crystals. Although there are many fiber fractures, there was no detectable load drops in the stress strain curve. The noise-limited smallest detectable load drops is 0.05 kgm. When we assume this value in our calculations, we arrive at a fiber strength in the matrix of 2722 MPa. This is about 70 percent of the virgin fiber tensile strength. It should be noted, however, that degradation of the fiber strength is known to occur during MMC processing, the "knockdown" effect.

2. Al_2O_3/NiAl

These specimens were extremely brittle and fracture occurred catastrophically such that no acoustic emission events could be recorded.

II. THERMAL STRESSES IN MODEL COMPOSITES CONTAINING GRADED COMPOSITION INTERMEDIATE LAYERS

A. PARAMETRIC STUDY

The SCS-6/Ti_3Al+Nb composite with functionally graded intermediate layers based on fiber and matrix properties was used for the parametric study. Both the interface layer thickness (t/a ratio) and the transition of material properties (gradation number, n) were investigated. The property gradation formula was given previously in Figure 2. Graded layer yield strengths were approximated using this property gradation formula. These yield strengths become very high as ceramic content increases, due to the very high yield strengths of ceramics. These high yield strength approximations magnified the effects of layer thickness and gradation number on constituent stresses, by allowing high stresses to be generated and maintained in the layers. This allowed clear examination of the trends by producing larger effects. However, the stresses predicted in the layers in this manner should be considered upper bounds and, therefore, conservative. The actual yield strengths of such cermet layers probably lie between these approximations and the matrix yield strength. The generated stresses would, therefore, also be lower.

CASE 1. SiC/Ti_3Al+Nb composite system with graded intermediate layer (t/a = 10 percent; n=1, 0.5 and 2)

Radial Stress

Radial stress in the fiber region, which is in compression, stays constant, Figure 8. The variation of stress level is less than 1 percent with changing radial location. However, the radial stress in this region for the composite systems with graded layers has an increasing tendency with decreasing gradation number. The stress levels vary from that of the baseline case (i.e., no graded layers) by 4.9 percent, 13.7 percent and 19 percent, for the cases of gradation number equal to 2, 1 and 0.5, respectively. The baseline case has a radial stress equal to -172 MPa at the center of the fiber.

Both in the graded layers and the matrix regions, the radial stress has a rising trend and is increased smoothly with increasing radial location.

The radial stress in the matrix region is not influenced by introducing the graded layers. In the interface boundary of the matrix and the outer graded layer at r = 0.695, the stress value is increased no greater than 6.4 percent, comparing to the baseline case.

Axial Stress

Axial stress in the fiber region, which is in compression, is constant, Figure 8. For the baseline case (no graded layer), the axial stress is equal to -535 MPa at the center of the fiber. The axial stress is deviated from that of the baseline case by -8.5 percent, -1.5 percent, and +3.8 percent, for the graded layer cases of graduation number equal to 2, 1, and 0.5, respectively.

The axial stress has a rising trend with increasing radial location in the matrix region. The stress level changes from 240 MPa at the matrix inner boundary ($r = 0.632$) to 423 MPa at the outer boundary ($r = 1$). Note that the axial stress at the outer boundary exceeds the matrix material yield strength (in this case, 371 MPa), indicating that matrix flow has occurred. Adding graded layers to the composite system has little effect on reducing the axial stress level in the matrix region; the axial stress is reduced only by 4.7 percent at the interface boundary of $r = 0.695$ for the best case of gradation number equal to 2.

The axial stress transition is largely improved with the introduction of graded layers. In the baseline case (i.e., no graded layers), due to the discontinuity of material between the fiber and the matrix, the axial stress is increased rapidly by 775 MPa (from -534 MPa to +241 MPa) with a state change from compression to tension at the interface boundary of $r = 0.632$. By adding graded layers, the transition of axial stress is becoming smoother at the interface region with increasing gradation number. The stress jump at the interface boundary is reduced, comparing with the baseline case, by 13 percent (675 MPa), 68 percent (247 MPa), and 96 percent (47 MPa) for gradation number equal to 0,5, 1, and 2, respectively. This implies that the thermal stress gradient resulting from thermal mismatch of the fiber and the matrix may become less severe by introducing the graded layers in the interface region.

However, most of the axial stress levels in the interface region ($0.632 < r < 0.695$) are higher than the baseline case without graded layers (e.g., 545 MPa for $n = 2$ vs. 283 MPa w/o graded layer at $r = 0.689$). Material failure may become a concern of the composite system while considering the thermal mismatch issue if the high stress values exceed the material yield strength of the graded layers.

The axial stress drop due to the material discontinuity at the interface boundary of the outer graded layer and the matrix ($r = 0.695$) is observed.

Hoop Stress

The hoop stress in the fiber region, which is in compression, stays constant, Figure 8. For the baseline case (no graded layer), the hoop stress is equal to -172 MPa at the center of the fiber. The hoop stress is deviated from that of the baseline case by 4.9 percent, 13.7 percent, and 19 percent, for the graded layer cases of gradation number equal to 2, 1, and 0.5, respectively.

The hoop stress remains quite stable in the matrix region; the maximum stress deviation is less than 9.2 percent. The stress level is decreasing slightly at the matrix outer boundary (from 297 MPa at r = 0.695 to 278 MPa at r = 1). Adding graded layers to the composite system has no effect on reducing the hoop stress level in the matrix region. The hoop stress is actually increased by 8.6 percent at the matrix outer boundary for the case of gradation number equal to 2. The increase of the hoop stress level is below the matrix material yield strength.

In the baseline case (i.e., no graded layers), due to the discontinuity of material between the fiber and the matrix, the hoop stress is increased by 448 MPa (from -171 MPa to +279 MPa) with a state change from compression to tension at the interface boundary of r = 0.632. The hoop stress transition is largely improved with the introduction of graded layers for the cases of gradation number equal to 1, and 2. The stress jump at the interface boundary is reduced, comparing with the baseline case, by 51 percent (221 MPa) and 95 percent (23 MPa), respectively. This implies that the thermal stress gradient resulting from thermal mismatch may become less severe by introducing graded layers in the interface region. However, for the graded layer case of gradation number equal to 0.5, the stress transition become worse where the stress jump is increased by 31 percent (588 MPa).

It should be noted that most of the hoop stress level in the interface region ($0.632 < r < 0.695$) are much higher than the baseline case without graded layers (e.g., 641 to 650 MPa vs. 294 MPa w/o graded layers). Interface material failure may become a concern of the composite system while considering the thermal mismatch issue if the graded layers have high yield strengths or low ductilities.

The hoop stress drop due to the material discontinuity at the interface boundary of the outer graded layer and the matrix (r = 0.695) is observed.

CASE 2. SiC/Ti_3Al+Nb composite system with graded intermediate layer (n=1; t/a=5, 10 and 15%

In this case the effect of intermediate layer thickness was studied. The radial stress component (Figure 9) within the fiber is compressive and rises smoothly with

increasing value of radius. As in CASE 1, radial stresses remain compressive as they transition the intermediate layer. The magnitude of the radial stress is not significantly affected by introducing the graded intermediate layer.

The axial stress component is also compressive within the fiber but rapidly rises to positive values within the graded layer. Although the change in stress with radial location is less marked when a graded intermediate layer is present, the peak stresses attained are higher and in the case where t/a=10% remain high into the matrix.

The hoop stresses have a similar distribution to those of the axial stresses. Increasing the t/a ratio tempers, somewhat, the rate of stress increase through the graded layer; however, the peak stresses are higher than the axial stresses. As with the axial stress at a t/a 10%, the hoop stresses are high even in the initial matrix layers raising the possibility of interface material failure.

B. FEM STUDY OF FABRICATED COMPOSITES

In this study, material parameters for an intermediate layer based on Ti-TiN-Ti were used in the model. The TiN content in this layer was decreased in steps of 10% i.e., (100% TiN), (90% TiN, 10% Ti) (80% TiN, 20% Ti)...etc. The property of the Ti adhesion layer was also factored into the model.

1. SiC/Ti_3Al composite system with Ti-TiN-Ti graded layers (t/a = 10 percent; n = 1)

Radial Stress

The radial stress in the fiber region, which is in compression, stays constant, Figure 10. The stress level at the center of the fiber is increased, compared with the baseline case with no graded layers, by 2.8 percent (i.e., -177 MPa vs. -172 MPa). Both in the graded layers and the matrix regions, the radial stress has a rising trend and is increased smoothly with increasing radial location. The radial stress in the matrix region is not influenced by introducing the graded layers.

Axial Stress

Axial stress in the fiber region, which is in compression, is a constant, Figure 10. For the baseline case (no graded layer), the axial stress is equal to -535 MPa at the center of the fiber. The axial stress is decreased from that of the baseline case by 1.6 percent for the composite system with graded layers.

The axial stress has a rising trend with increasing radial location in the matrix region. The stress level changes from 241 MPa at the matrix inner boundary (r = 0.632) to 423 MPa at the outer boundary (r = 1). Note that the axial stress at the outer boundary exceeds the matrix material yield strength in this

case, 371 MPa, indicating that matrix flow has occurred. Adding graded layers to the composite system has little effect on reducing the axial stress level in the matrix region; the axial stress is reduced only by 2.2 percent at the interface boundary of r = 0.695.

The axial stress transition is improved with the introduction of graded layers. In the baseline case (i.e., no graded layers), due to the discontinuity of material between the fiber and the matrix, the axial stress is increased rapidly by 775 MPa (from -534 to +241 MPa) with a state change from compression to tension at the interface boundary of r = 0.632. By adding graded layers, the transition of axial stress is becoming smoother at the interface region.

However, some of the axial stress levels in the interface region ($0.632 < r < 0.695$) are higher than the baseline case without graded layers (e.g., 370 MPa with graded layers vs. 283 MPa with no graded layers at r = 0.695). Interface material failure may become a concern of the composite system while considering the thermal mismatch issue if the graded layers have high yield strengths or low ductilities.

A drop in the axial stress is observed due to the material discontinuity at the interface boundary of the outer graded layer and the matrix (r = 0.695).

Hoop Stress

Hoop stress in the fiber region, which is in compression, stays as a constant, Figures 10. For the baseline case (no graded layer), the hoop stress is equal to -172 MPa at the center of the fiber. The hoop stress is increased from that of the baseline case by 2.8 percent for the composite system with graded layers.

The hoop stress stays quite stable in the matrix region; the stress deviation is less than 9.2 percent. The stress level is decreasing slightly at the matrix outer boundary (from 297 MPa at r = 0.695 to 278 MPa at r = 1). Adding graded layers to the composite system has no effect on reducing the hoop stress level in the matrix region; the hoop stress is actually increased by 4.1 percent. The increase of the hoop stress in the matrix region will not influence the composite system since the stress level is below the matrix material yield strength.

In the baseline case (i.e., no graded layers), due to the discontinuity of material properties between the fiber and the matrix, the hoop stress is increased by 450 MPa (from -171 to +279 MPa) with a state change from compression to tension at the interface boundary of r = 0.632. The hoop stress transition is improved with the introduction of graded layers. The stress jump at the interface boundary is reduced, comparing with the baseline case, by 22 percent (350 MPa). This implies that the thermal stress resulting from

thermal mismatch may become less severe by introducing graded layers in the interface region.

It should be noted that the hoop stress level in the interface region ($0.632 < r < 0.695$) is sometimes higher than the baseline case without graded layers (e.g., 411 MPa with graded layers vs. 294 MPa with no graded layers at $r = 0.695$). Interface material failure may become a concern of the composite system while considering the thermal mismatch issue if the graded layers have yield strengths and/or low ductilities.

The hoop stress drop due to the material discontinuity at the interface boundary of the outer graded layer and the matrix ($r = 0.695$) is observed.

2. **Al_2O_3/NiAl Composite System with Graded Intermediate Layer (t/a = 10 percent; n = 1)**

Radial Stress

Radial stress in the fiber region, which is in compression, is constant, Figure 11. The stress level at the center of the fiber is significantly increased comparing with the baseline case with no graded layers, by 35 percent (i.e., -183 vs. -247 MPa).

In the matrix region, the radial stress has a rising trend, numerically, and is increased smoothly with increasing radial location. However, the radial stress changes rapidly within the graded layers, from -244 MPa at the inner boundary, to -146 MPa, the outer boundary. That would be a 126 percent stress jump increase comparing to the baseline case without graded layers.

The radial stress in the matrix region is not influenced by introducing the graded layers.

Axial Stress

Axial stress in the fiber region, which is in compression, is constant, Figure 11. For the baseline (no graded layer), the axial stress is equal to -602 MPa at the center of the fiber. The axial stress is increased from that of the baseline case by 6.4 percent for the composite system with graded layers.

The axial stress has a rising trend with increasing radial location in the matrix region. For the baseline case, the stress level changes from 280 MPa at the matrix inner boundary ($r = 0.632$) to 480 MPa at the outer boundary ($r = 1$). Note that the axial stress at the outer boundary exceeds the matrix yield strength (in this case, 380 MPa). This indicates that matrix flow has taken place. Adding graded layers to the composite system has little effect on reducing the axial stress level in the matrix region; the axial stress is reduced only by 5 percent at the interface boundary of $r = 0.695$.

The axial stress transition is significantly improved with the introduction of graded layers. In the baseline case (i.e., no graded layers), due to the discontinuity of material between the fiber and the matrix, the axial stress is increased rapidly by 881 MPa (from -601 to +280 MPa) with a state change from compression to tension at the interface boundary of r = 0.632. By adding graded layers, the transition of axial stress is smoother at the interface region. The stress jump at the interface boundary is reduced, comparing with the baseline case, by 56 percent (385 MPa). This implies that the thermal stress gradient resulting from thermal mismatch of the fiber and the matrix may become less severe by introducing the graded layers in the interface region.

However, most of the axial stress levels in the interface region ($0.632 < r < 0.695$) are higher than the baseline case without graded layers (e.g., 984 MPa with graded layers vs. 309 MPa with no graded layers at r = 0.675). Interface material failure may become a concern of the composite system while considering the thermal mismatch issue if the graded layers have high yield strengths and/or low ductilities. The FEM analysis does show that in such cases this composite system may not survive due to the excessive high axial stress occurring in the graded layers. An axial stress drop due to the material discontinuity at the layer-matrix interface boundary layer and the (r = 0.695) is observed approaching the boundary.

Hoop Stress

Hoop stress in the fiber region, which is in compression, is constant, Figure 11. For the baseline case (no graded layer), the hoop stress is equal to -183 MPa at the center of the fiber. The hoop stress is increased from that of the baseline case by 35 percent for the composite system with graded layers.

The hoop stress stays as a constant in the matrix region. The stress level increases slightly with increasing radial location towards the matrix outer boundary (from 298 MPa at r = 0.695 to 310 MPa at r = 1). Adding graded layers to the composite system has no effect on reducing the hoop stress level in the matrix region; the hoop stress is actually increased by 4.6 percent. This increase of the hoop stress in the matrix region will not influence the composite system since the stress level is below the matrix material yield strength.

In the baseline case (no graded layers), due to the discontinuity of material between the fiber and the matrix, the hoop stress is increased by 476 MPa (from -181 to +295 MPa) with a state change from compression to tension at the interface boundary of r = 0.632. The hoop stress transition is improved with the introduction of graded layers. The stress jump at the interface boundary (i.e., 398 MPa) is reduced by 16 percent compared to the baseline case. This implies that the thermal stress gradient resulting from thermal

mismatch may become less severe by introducing graded layers in the interface region.

However, it should be noted that of the hoop stress levels in the interface region ($0.632 < r < 0.695$) are often much higher than in the baseline case without graded layers (e.g., 1245 MPa with graded layers vs. 300 MPa with no graded layers at $r = 0.665$). Interface material failure becomes a serious concern of this composite system since the FEM analysis indicates that the high stress values in the graded layers exceed the material yield strength.

A considerable drop of the hoop stress due to the material discontinuity at the interface boundary of the outer graded layer and the matrix ($r = 0.695$) is observed.

Fabrication of Model Composite with Graded Intermediate Layer

Multi-Layer Stacks on Flat Alumina Substrates

A number of stacks were tried. Two of the most successful multilayer designs, 1 and 2, are shown in Figure 12. Both of these stacks rely on using alternating layers of Ni, Al and Al_2O_3 in varying thicknesses in order to effectively match the two CTE's. Both of the stack designs were fabricated on four inch diameter sapphire wafers that were cleaned using a standard semiconductor cleaning technique. The wafers were then cut into sections for testing. Some sections were examined by SEM and others were thermally cycled up to 1050°C in argon atmosphere, cooled and then examined visually and by SEM. No cracks, delamination, or degradation were observed in the SEM. Visually, the films appear to show no degradation.

Co-evaporated Al_2O_3 and Ni layers were also deposited onto sapphire wafers to thicknesses up to four microns using thin Ni layers for adhesion (layer design 3). These were also cycled up to 1050°C in argon and also show no cracking.

Multi-Layer Stacks on Fibers

1. SCS-6/Ti_3Al+Nb

The three magnetrons were fitted with three different cathodes, and a range of experiments were done to calibrate deposit thickness of different speed and power conditions. Magnetron cathodes that have been calibrated include Ti, TiN (deposited by reactive sputtering), and alpha-2 alloy (titanium aluminide).

The stack tried first on SCS-6 fiber was a graded composition consisting of : SiC (fiber): Ti-TiN (Gradually decreasing to Ti) -Ti : Ti_3Al+Nb. Various permutations of this multilayer stack design were deposited onto

SCS-6 using the reel-to-reel system. These permutations included a series of thicknesses as well as variation in the coating rates. Multiple passes were tried using high speeds and low deposition rates as well as low speed single passes and it was found that the film microstructure was critically dependent on the deposition rate. Generally, a finer microstructure tends to occur on fibers coated in multiple passes.

Three thicknesses were deposited, 1.8 micron, 4.5 micron and 14.5 micron. In each case approximately 1.5 continuous meters of fiber was coated. The matrix layer used in the test was about five microns and the thermal cycle included heating to 1050°C in vacuum with a dwell time of 30 minutes followed by cooling to room temperature. The above conditions were chosen to simulate the consolidation cycle. Optical and SEM examination indicated that graded layers having a thickness of about 4.5 microns or more were effective in reducing matrix cracking in this composite system. Examples of the SEM micrographs are shown in Figures 13, 14, 15, and 16. The results are summarized in Table 9.

2. Al_2O_3/NiAl

A graded coating based on Ni-Al_2O_3-NiAl composition was developed for use in Al_2O_3/NiAl composite. The coating was deposited by cylindrical magnetron sputtering and had the following configuration:

1. 800 Angstroms of Ni-Al_2O_3 used as an adhesion layer
2. 1.2 Microns of Al_2O_3
3. 0.4 Micron NiAl
4. 0.8 Micron Al_2O_3
5. 0.8 Micron NiAl
6. 0.4 Micron Al_2O_3
7. 1.2 Microns NiAl

The NiAl was deposited by co-depositing Ni and Al (50/50 a/o)

This configuration was based on linearly varying the composition of the coating between the fiber and matrix (gradation index, n=1). The experimental thickness of the coating agrees with that estimated from measured sputtering rates of the various materials. The outer NiAl layer of the coating (1.2 microns) can be considered as a thin matrix situation. Figure 17 shows a section through as deposited graded coating before and after thermal cycling.

Microscopic examination of the as-coated fibers showed no cracks in the film. This examination was done on fibers coated in two separate experimental runs.

Fibers were subjected to a heating cycle of 1100°C for one hour in vacuum followed by a cool down to room temperature. Microscopic examination of the coating over six inch length fibers showed no cracking (or deformation) in the coating upon the thermal exposure. Figures 18 shows the absence of cracking in the surface of coated fiber before and after exposure to a fabrication thermal cycle.

Interface Shear Strength of Coated Fiber Systems

A. SCS-6/Ti_3Al+Nb

Disappointing results were obtained when machining coated SCS-6/Ti_3Al+Nb test specimens from the HIP bonded plates. Inadequate bonding was achieved which resulted in parting at the bond line during machining. The reasons for inadequate bonding are not clear. The same technique, albeit at lower bonding temperatures, was successful in earlier in-house studies of SCS-6/Ti-64. Inadequate surface cleaning prior to bonding or imperfect EB weld sealing are possible causes of the problem. Since fiber damage occurred during the machining attempts, remnant

samples of virgin coated fiber will be forwarded to NASA-LeRC for bonding and fiber push-out tests.

2. Al_2O_3/NiAl

Bonded sapphire/NiAl samples presented problems in machining acoustic emission test specimens; fracture and "chipping" of the samples was experienced so that suitable test specimens could not be made. In view of the results in testing uncoated sapphire/NiAl specimens, the present samples will be sent to NASA-LeRC for fiber push out tests.

SUMMARY AND CONCLUSIONS

A. Finite Element Analyses

1. The magnitude of the thermally induced fabrication residual stresses are satisfactorily calculated using the 2-D finite element analysis for the axisymmetric model.

2. For the SCS-6/Ti_3Al+Nb system (no intermediate layer) both the hoop and axial stresses increase markedly at the fiber-matrix interface. The hoop stress remains below the yield stress of the Ti_3Al+Nb matrix. However, the axial stresses exceed the yield stress though remain below the ultimate tensile stress.

3. For the SCS-6/Ti-TiN-Ti/Ti_3Al+Nb (thin matrix) system the intermediate Ti-TiN-Ti layer modifies the hoop and axial stress distribution within the intermediate layer but the magnitude of the stresses in the Ti_3Al+Nb matrix remains essentially unchanged. The stresses generated within the graded layers were predicted to be very high due to the high layer yield strengths assumed in upper bound approximations.

4. For the case where a thick Ti_3Al+Nb marix layer and low volume fraction of fiberis employed with the intermediate Ti-TiN-Ti layer, there is a significant reduction in hoop and axial stresses and both remain below the yield strength of the matrix.

5. For the SCS-6/Ti_3Al+Nb system employing graded Ti-TiN-Ti intermediate layers, the effect of grading is to reduce the hoop and axial stress gradients within the intermediate layer. However, both stresses attain maximum values which exceed those when no graded intermediate layer is used. This occurs both when the intermediate layer thickness (t/a) and gradation number (n) is varied.

6. The stress distribution for the Al_2O_3/NiAl system (no intermediate layer) parallels that for SCS-6/Ti_3Al+Nb. There is a marked increase in hoop and axial stresses across the fiber-matrix interface. The hoop stress remains below the yield stress of NiAl, but the axial stress rises above it. For NiAl, therefore, matrix cracking is predicted.

7. For the Al_2O_3/NiAl system with a graded intermediate layer the hoop and axial stress gradients in the intermediate layer are reduced over those occurring when no graded interlayer is used. However, as was the case for the SCS-6/Ti_3Al+Nb system with intermediate layer, the maximum stresses attained are much higher with the result that matrix cracking will be exacerbated.

B. Fiber Coatings

1. Graded intermediate layer coatings have been successfully deposited on SCS-6 and sapphire fibers using a multi-target reel-to-reel sputtering system.

2. Thermal cycling of Ti_3Al+Nb deposited on SCS-6 fiber results in severe cracking of the coating.

3. A graded intermediate Ti-TiN-Ti layer can prevent cracking of the Ti_3Al+Nb matrix. A Ti-TiN-Ti thickness of 4.5 μm resulted in no cracking. Cracking of Ti_3Al+Nb was observed for both thinner (1.8μm) and thicker (14.5μm) graded intermediate layers.

4. For the sapphire/NiAl system, an intermediate layer consisting of a Ni bond coat and a graded deposit of Al_2O_3-NiAl appears to resist cracking when the coated fiber is thermally cycled to 1100°C.

C. Acoustic Emission Testing

1. Acoustic emission tests were not wholly successful for determining interfacial stresses using the test specimens employed in this study.

2. Load drops could not be detected for the SCS-6/Ti_3Al+Nb system (no intermediate layer) and this was attributed to too high a ratio of matrix to fiber in the cross-section. Bonding difficulties prevented testing specimens when the graded intermediate layer was employed.

3. Brittle failure in tension the Al_2O_3/NiAl specimens precluded the ability to detect load drops that would arise due to successive fracture occurring in the fiber.

REFERENCES

1. Hirano, T., Teraki, J., and Yamada, T., "On the design of Functionally Gradient Material," Proc. 1st Int'l Symp. FGM, 5-10 (1990).

2. Ishikawa, T., "Thermal Deformation and Thermal Stress of FGM Plates under Steadily Graient Temperature Field," Proc. 1st Int'l Symp. FGM, 11-16(1990).

3. Arnold, Arya, V.K., and Melis, M.E., "Elastic/Plastic Analyses of Advanced Composites Investigating the Use of Graded Layer Concept in Reducing Residual Stresses Resulting from Processing," NASA TM-103204(1990).

4. Clough, R.B., Biancianello, F.S., Wadley, H.N.G. and Kattner, V., "Fiber and Interface Fracture in Single Crystal Aluminum - SiC Fiber Composites," Met. Trans., A, 20A, 2747-2757 (1990).

TABLE 1
MODEL DIMENSIONS AND MATERIAL SYSTEMS

Dimensions							Model Fiber Volume Fraction
TSK	**rf**	**rc1**	**rc2**	**rc**	**rm**	**L**	
TSK12	0.632	---	---	---	1	1	.40
TSK13	0.632	---	---	---	1	1	.40
TSK14	0.632	---	---	0.695	1	1	.40
TSK15	0.632	0.645	0.682	0.695	1	1	.40
TSK16	0.632	0.645	0.682	0.695	1.58	1	.16

Materials			
Fiber	**Matrix**	**Intermediate Layer**	
F2	M2	---	F1: Al_2O_3
F1	M1	---	M1: NiAl
F2	M2	Ti-TiN-Ti	F2: SiC
F2	M2	Ti-TiN-Ti	M2: Ti_3Al+Nb
F2	M2	Ti-TiN-Ti	

TABLE 2
ROOM TEMPERATURE/MATERIAL PROPERTIES

	E (MPa)	α (μ Meter/Meter°C)	υ	σ_y (MPa)	H_s (MPa)	σ_{ult} (MPa)
Al_2O_3	413E3	1.63	0.30	2067	---	---
NiAl	187E3	2.13	0.30	379	12,953	---
SiC	400E3	1.09	0.25	4134	---	---
Ti_3Al	110E3	2.78	0.26	371	22,944	489 (est)
Ti (RMI 40)	103E3	2.67	0.34	276	937	345
TiN	80E3	1.96	0.30	3445	---	---
Ti+TiN Volume (2:3)	89E3	2.24	0.32	---	---	---

E: Elastic Modulus
α: Coefficient of Thermal Expansion
υ: Poisson's Ratio
σ_y: Yield Strength
H_s: Hardening Slope
σ_{ult}: Ultimate Strength

TABLE 3
MATERIAL PROPERTIES VERSUS TEMPERATURE

1. Elastic Modulus (MPa)

Temp. (°C)	24	200	425	600	650	816
Al_2O_3	413E3					
NiAl	187E3	187E3		165E3	---	(155E3)
SiC	400E3	392E3	383E3	376E3	374E3	368E3
Ti_3Al	110E3	100E3	96E3	86E3	68E3	45E3
Ti (RMI 40)	103E3					
TiN	80E3	78E3	76E3	73E3	72E3	70E3
Ti+TiN Volume (2:3)	89E3					

2. Coefficient of Thermal Expansion (micro meters/meter/°C)

Temp. (°C)	24	200	425	600	650	816
Al_2O_3	1.63	1.82	2.22	2.42	---	2.49
NiAl	2.13	2.24	2.47	2.61	---	2.70
SiC	1.09	1.12	1.21	1.29	1.32	1.38
Ti_3Al	2.78	2.89	3.17	3.25	3.28	3.42
Ti (RMI 40)	2.67	2.74	2.92	3.06	3.11	3.11
TiN	1.96	2.44	2.78	2.97	3.02	3.13
Ti+TiN Volume (2:3)	2.24	2.56	2.83	3.01	3.06	3.12

3. Hardening Point Characteristics for Bilinear Plasticity Simulation (Units in MPa)

Temp. (°C)		24	200	316	425	538	600	650	816
NiAl	σ_y	380	335	---	264		150	---	58
	H	13E3	10E3	---	2.4E3		0.8E3	---	01.E3
Ti_3Al	σ_y	371	407	---	370		291	269	165
	H	23E3	3E3	---	2E3		1.3E3	0.7E3	---
Ti	σ_y	276	---	124	103	76			
(RMI 40)	H	.9E3	---	.1E3	.1E3	---			

σ_y: Yield Stress
H: Hardening Slope

TABLE 4
RESIDUAL STRESS ANALYSIS FOR PARAMETRIC STUDY

Layer	Location (r)	Task	Radial Stress		Axial Stress		Hoop Stress	
			Elastic MPa	Elastic Plastic MPa	Elastic MPa	Elastic Plastic MPa	Elastic MPa	Elastic Plastic MPa
Fiber	0.0 (Inner)	TSK12	-226	-158	-624	-457	-226	-158
		TSK13	-630	-181	-1397	-601	-630	-181
		TSK14	-209	---	-587	---	-209	---
		TSK15	-210	-162	-590	-502	-210	-162
		TSK16	-325	-278	-1176	-1135	-325	-278
Fiber	0.632 (Outer)	TSK12	-223	-156	-623	-457	-224	-156
		TSK13	-622	-180	-1395	-600	-625	-156
		TSK14	-206	---	-586	---	-206	---
		TSK15	-207	-160	-589	-501	-207	-160
		TSK16	-321	-274	-1174	-1133	-321	-274
Matrix	0.632 (Inner)	TSK12	-223	-156	414	220	520	278
		TSK13	-622	-180	927	274	1449	293
Matrix	0.695 (Inner)	TSK14	-166	---	425	---	477	---
		TSK15	-166	-133	424	287	472	302
		TSK16	-277	-244	232	122	405	221
Matrix	1.0 (Outer)	TSK12	<1	<1	414	314	298	218
		TSK13	1	<1	927	479	831	310
		TSK14	<1	---	425	---	311	---
		TSK15	<1	<1	424	425	310	287
Matrix	1.0 (Middle)	TSK16	-99	-96	233	236	232	224

TABLE 4
RESIDUAL STRESS ANALYSIS FOR PARAMETRIC STUDY

Layer	Location (r)	Task	Radial Stress		Axial Stress		Hoop Stress	
			Elastic MPa	Elastic Plastic MPa	Elastic MPa	Elastic Plastic MPa	Elastic MPa	Elastic Plastic MPa
Matrix	1.58 (Outer)	TSK16	<1	<1	233	236	133	128
Inner-Ti Layer	0.632 (Inner)	TSK14	-206	---	170	---	249	---
		TSK15	-207	-160	381	111	471	131
		TSK16	-321	-274	175	-36	378	37
Inner-Ti Layer	0.645 (Outer)	TSK14	-197	---	170	---	241	---
		TSK15	-194	-154	381	116	462	133
		TSK16	-307	-268	175	-31	369	40
Mid-TiN Layer	0.645 (Inner)	TSK14	-197	---	170	---	241	---
		TSK15	-194	154	60	91	121	142
		TSK16	-307	-268	-100	-79	50	73
Mid-TiN Layer	0.683 (Outer)	TSK14	-173	---	-170	---	217	---
		TSK15	-176	138	60	91	107	129
		TSK16	-288	-249	-100	-79	35	54
Outer-Ti Layer	0.683 (Inner)	TSK14	-173	---	170	---	217	
		TSK15	-177	-138	378	133	431	150
		TSK16	-288	-249	172	-12	334	58

TABLE 4
RESIDUAL STRESS ANALYSIS FOR PARAMETRIC STUDY

Layer	Location (r)	Task	Radial Stress		Axial Stress		Hoop Stress	
			Elastic MPa	Elastic Plastic MPa	Elastic MPa	Elastic Plastic MPa	Elastic MPa	Elastic Plastic MPa
Outer-Ti Layer	0.695 (Outer)	TSK14	-166	---	170	---	210	---
		TSK15	-166	-133	378	138	427	151
		TSK16	-277	-244	172	-5	331	62

NOTES:

TSK12 F2/M2 (No intermediate layers)
TSK13 F1/M1 (No intermediate layers)
TSK14 F2/Ti-TiN-Ti/M2 (ONE volume averaged property intermediate layer, THIN matrix)
TSK15 F2/Ti-TiN-Ti/M2 (THREE actual intermediate layers, THIN matrix, fiber v/o = 40
TSK16 F2/Ti-TiN/Ti/M2 (THREE actual intermediate layers, THICK matrix, fiber v/o = 16

F1/M1 = Aluminum Oxide (Al_2O_3)/NiAl
F2/M2 = SiC/Ti_3Al+Nb

TABLE 5
SPUTTERING CONDITIONS AND COMPOSITIONS* OF MATRIX FILMS DEPOSITED ON SAPPHIRE

	Power (Watts)	Rate A°/Min	Composition (Atom %)				
			Ti	Al	Nb	Ni	Al
A. Ti_3Al+Nb							
Target (Nominal)	---	---	65	24	11	---	---
Run 1	50	42	62.9	21.6	15.6	---	---
Run 2	150	150	63.1	21.5	15.4	---	---
Run 3	250	217	63.1	21.8	15.2	---	---
B. NiAl							
Target (Nominal)	---	---	---	---	---	50	50
Run 4	50	66.7	---	---	---	50.95	49.05
Run 5	100	83.3	---	---	---	49.67	50.33

* EDAX Analysis

TABLE 6
FLATNESS MEASURMENTS AND RESIDUAL STRESS FOR COMPOSITE FILMS ON SAPPHIRE

Sample No.	Film Composition	Substrate Thickness (μm)	Substrate Radius Before Exposure (M)	Thermal Exposure	Substrate Radius After Exposure	Residual Stress (Mpa)
0	**NA-12 NiAl**	**2.0**	**—**	**10 min 1050°C**	**19**	158
1	NA-11 NiAl	2.9	>100	10 min 1050°C	19	110
2	NA-11 NiAl	2.9	>100	10 min 1050°C	32	62
3	NA-12 NiAl	2.0	---	10 min 1050°C	19	158
4	NA-13 NiAl	1.0	---	10 min 1050°C	38	158
5	NA-14 Ti_3Al	2.8	---	10 min 1000°C	9	235
6	NA-14 Ti_3Al+Nb	2.8	9	None	---	234
6b	NA-14 Ti_3Al+Nb	2.8	11	10 min 1000°C	9	234
7	NA-15 Ti_3AlNb	1.4	---	10 min 1000°C	16	262
8	NA-15 Ti_3Al+Nb	1.4	60	None	---	69
8b	NA-15 Ti_3Al+Nb	1.4	60	10 min 1000°C	15	282

TABLE 7
ACOUSTIC EMISSION TEST RESULTS FOR SCS-6/Ti_3Al+Nb

Fiber Segments	AJ2 (mm)	AK1 (mm)	AK2 (mm)
1	0.48	0.49	2.18
2	0.97	0.49	5.08
3	1.94	3.87	19.85
4	3.66	7.75	26.63
5	4.84	21.30	
6	26.15	26.68	
7	43.08		
AE Gage Length (mm)	80.37	60.53	74.07
Actual Fiber Length (mm)	76.45	72.28	76.15
% Difference	5.1	20.0*	7.0
1c (mm)	0.48	0.49	~
No. of Flagged AE Events	11	10 - 11	7
Stress at Failure (kgm)	1030	910	1019

* Fiber was bent in AK1

TABLE 8
FIBER DIMENSIONS OF ACOUSTIC EMISSION TESTES SCS-6/Ti_3Al+Nb OBTAINED BY ACID DISSOLUTION OF THE MATRIX

Segments found in Long Broken End	AJ2	AK1	AK2
	0.64	0.81	4.70
	2.11	5.53	62.23
	4.90	54.61	
	6.10		
	53.34		
Total (mm) actual before acid etching (inches)	67.08	60.15**	
	67.18	67.01	
Comments - Microscopic Examiniation	Possible transverse cracks in the long segment***	Fiber skin is badly cracked. Possible numerous transverse cracks.	Similar to AJ2

* Only long position of broken specimen was used to obtain above results.

** Fiber was found bent in AK1.

*** Microscopic examination is very difficult. The acoustic emission results are more reliable based on accountability of total specimen length. Only one side of broken specimens was etched.

TABLE 9
VISUAL EVALUATION OF CRACKING FOR VARIOUS COMBINATIONS ON SCS-6 FIBER

Layer Combination	Total Thickness of Graded Layer (microns)	Cracking Density over 80 x 100 μ area observed at x 1000
Ti_3Al+Nb	4.5	severe cracking - 7 connected cracks
Ti-TiN-Ti/Ti_3Al+Nb	1.8	α-2 cracked and peeled off
Ti-TiN-Ti/Ti_3Al+Nb	4.5	coating performs well - no cracks
Ti-TiN-Ti/Ti_3Al+Nb	~ 15	single isolated crack

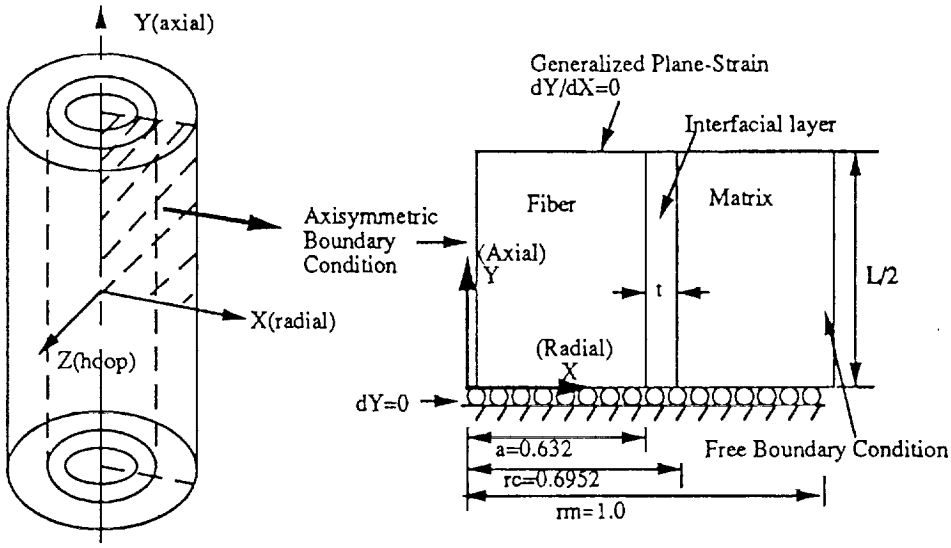

Figure 1. Model Single Fiber Composite

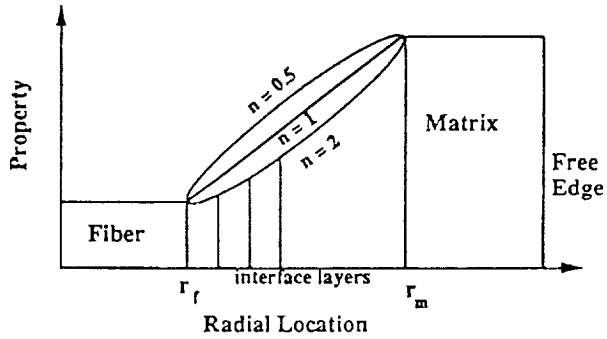

$$P = P_f(T) + (P_m(T) - P_f(T)) \left(\frac{r-r_f}{r_m-r_f}\right)^n$$

n - gradation number
P - Interface layer property: α, E, σ_y, H (hardening slope)
$P_f(T)$ - Fiber property as function of temperature
$P_m(T)$ - matrix property as function of temperature
r - radial location of mid-point of interface layer
$r_f = a$ - outer fiber radius, $t = r_m - r_f$.
r_m - inner matrix radial location

Figure 2. Property Gradation Formula

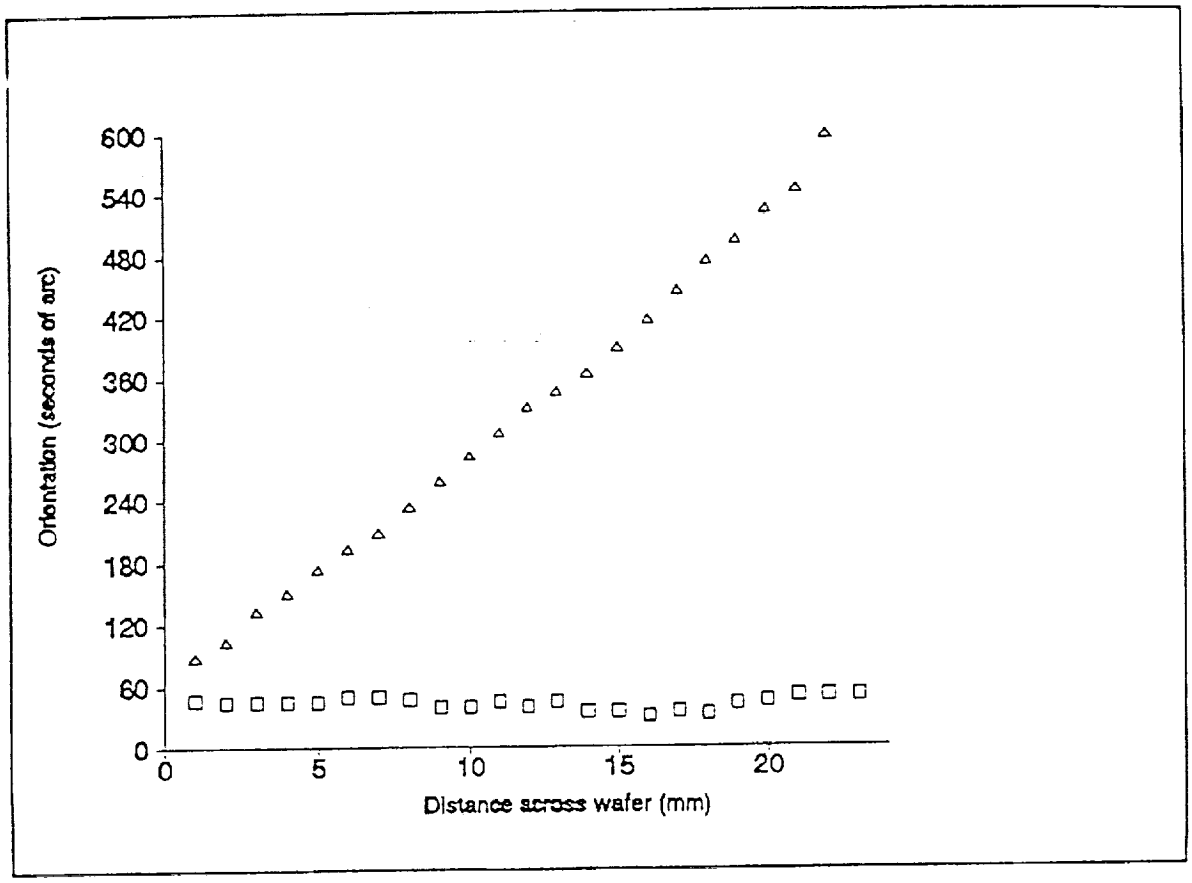

Bottom Trace:	Before growth
Top Trace:	After firing for 10 minutes at 1000°C
Film thickness:	2.8 μm
Final radius of curvature:	9 meters (film side concave)
Stress:	2.34 x 10^3 Mpa

Figure 3. Curvature Change of Sapphire Wafer with Ti_3Al Film Deposit (Wafer 5)

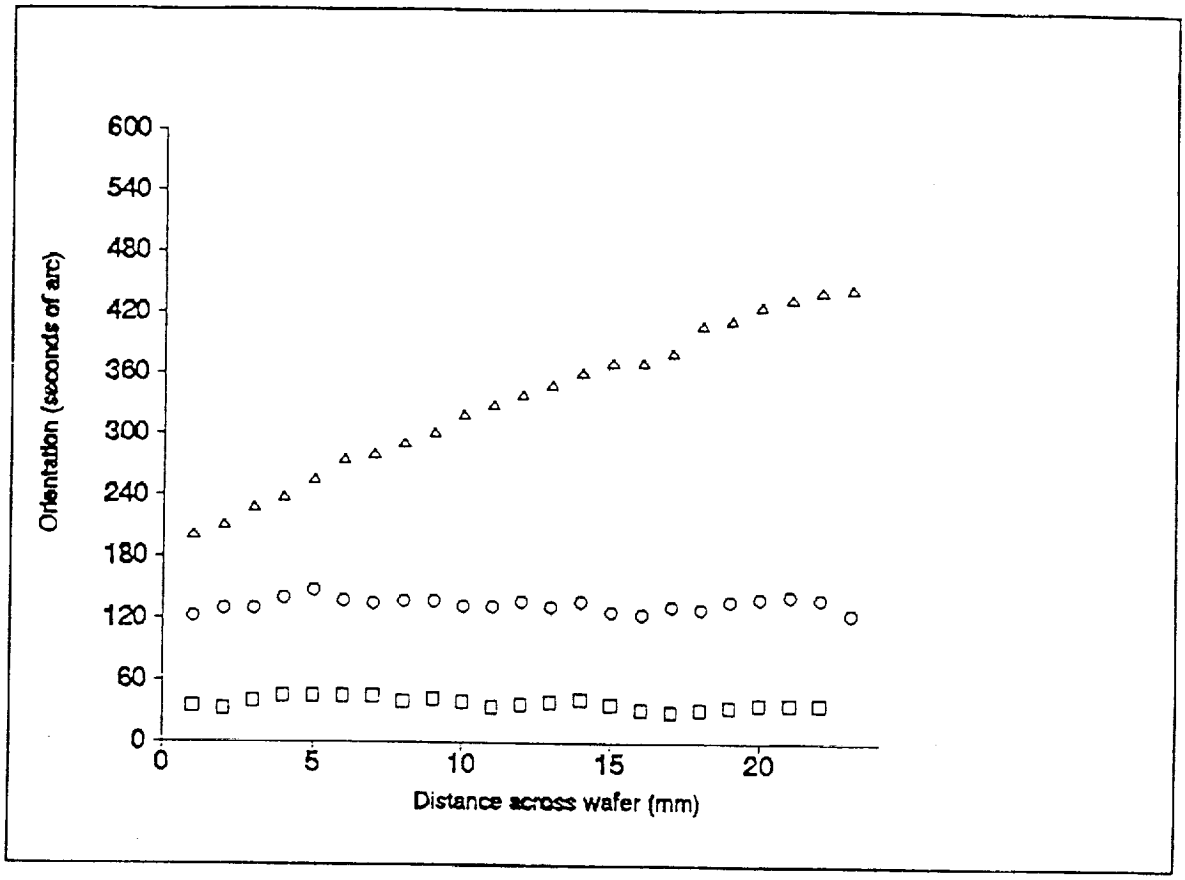

Bottom Trace:	Before growth
Middle Trace:	After deposition; before firing
Top Trace:	After firing for 10 minutes at 1050°C
Film thickness:	2.9 μm
Final radius of curvature:	19 meters (film side concave)
Stress:	1.1 x 10^3 Mpa

Figure 4. Curvature Change of Sapphire Wafer with NiAl Deposit (Wafer 1)

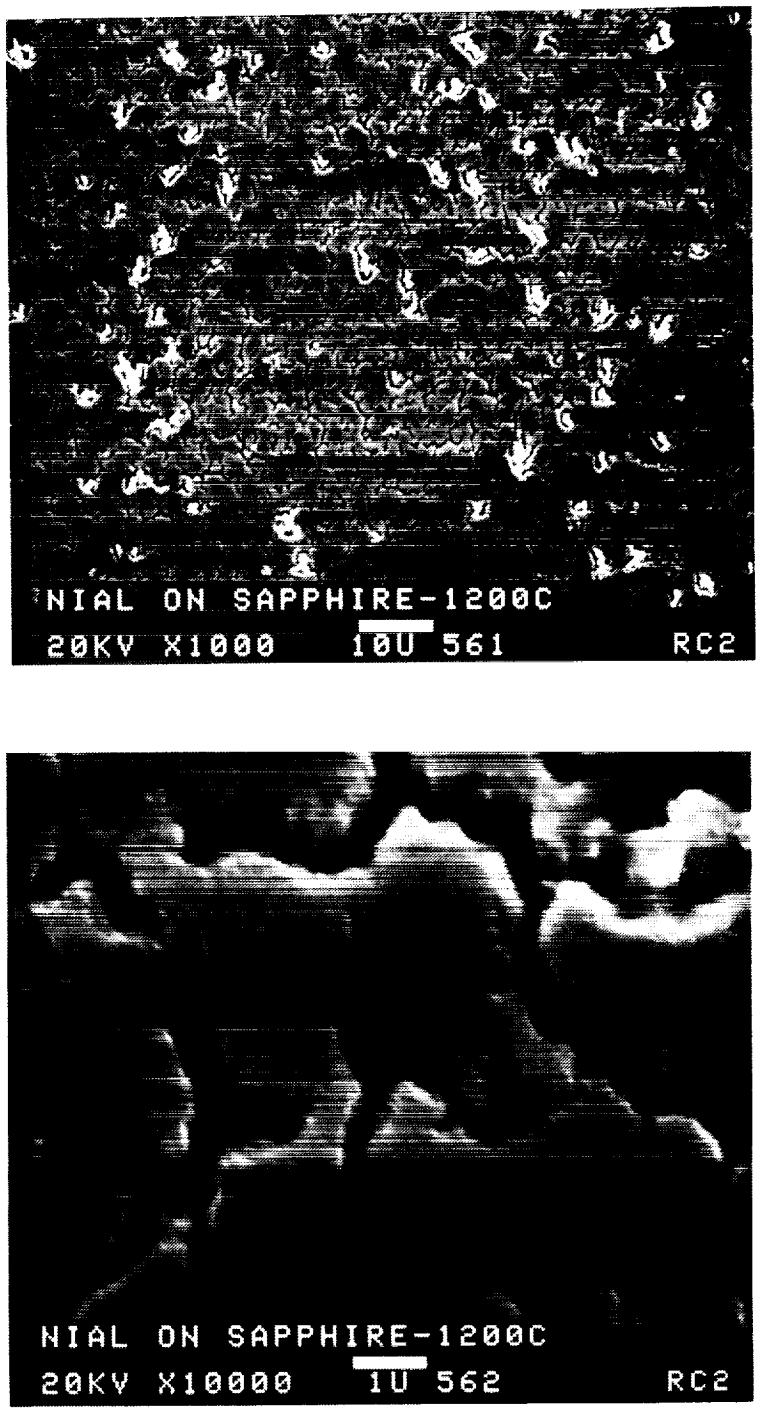

Figure 5. Thermal Crack Appearance of NiAl on Sapphire Wafer (Sample NA-12)

Figure 6. Thermal Crack Appearance of Ti_3Al+Nb on Sapphire Wafer (Sample NA-15)

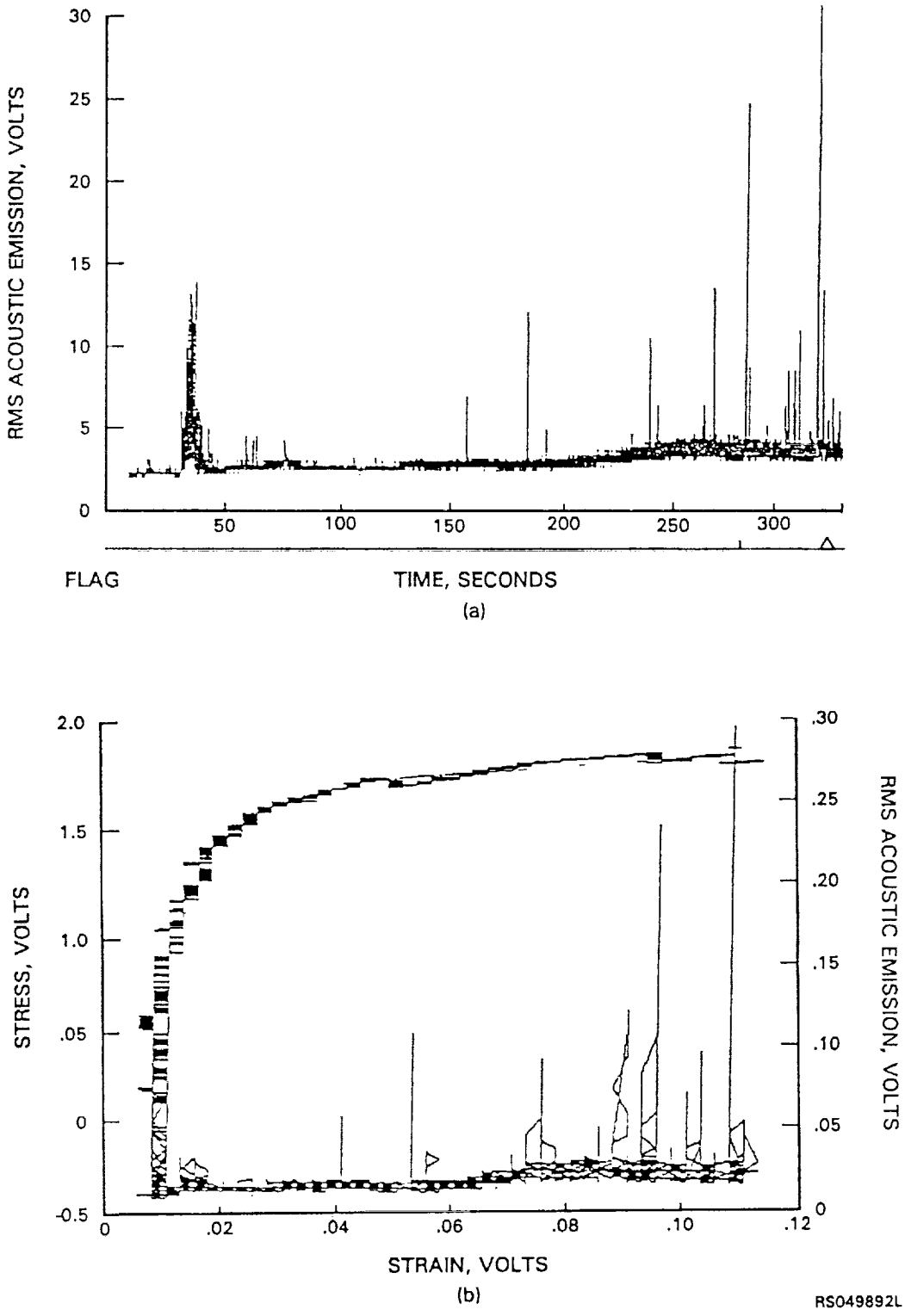

Figure 7. Examples of Acoustic Emission Recording SCS-6/Ti_3Al+Nb with No Graded Intermediate Layer a) Acoustic Emission vs. Time b) Stress vs. Strain and Acoustic Emission vs. Strain

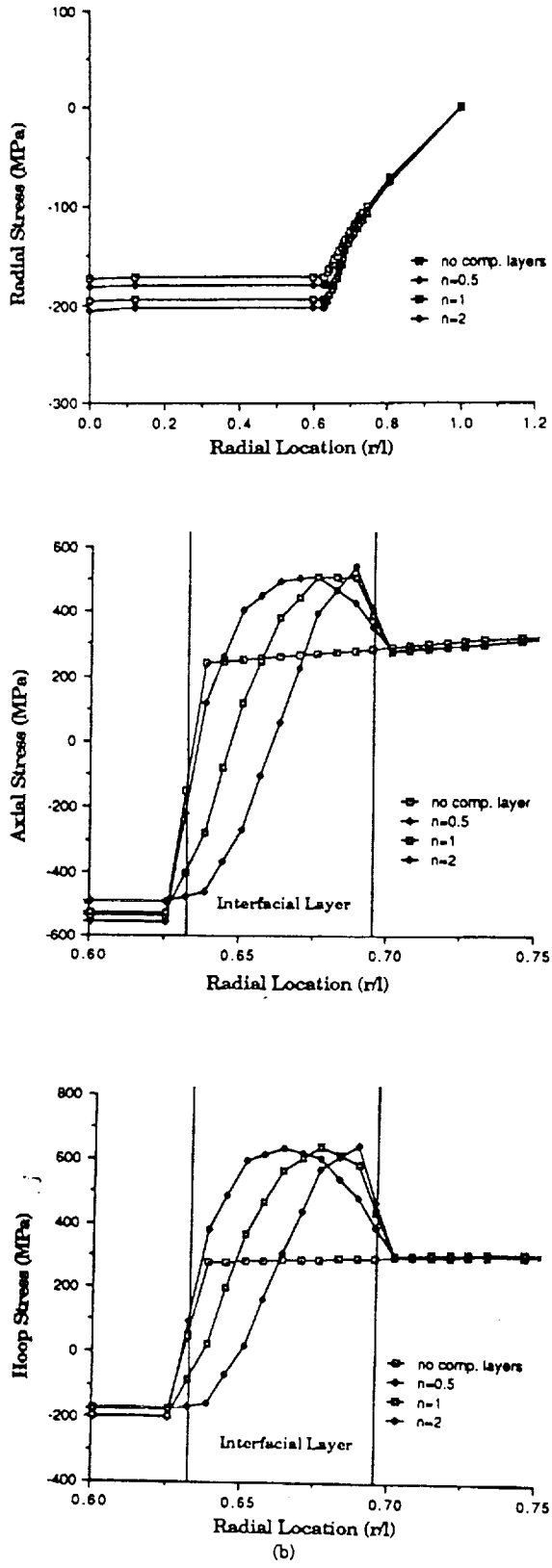

Figure 8. Radial, Axial and Hoop Stresses for SCS-61/Ti_3Al+Nb Showing Effect of a Graded Intermediate Layer (Parametric Study) t/a = 10%; n = 0.5, 1 and 2

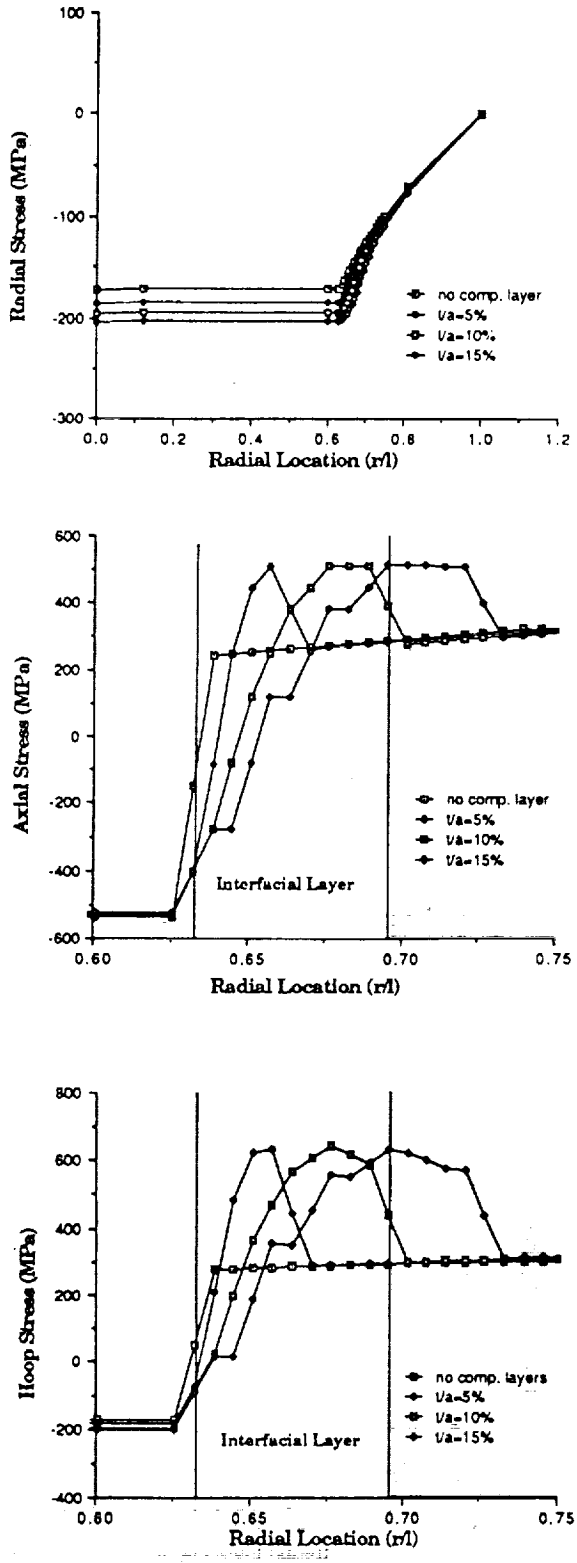

Figure 9. Radial, Axial and Hoop Stresses for SCS-6/Ti_3Al+Nb Showing Effect of n = 1; t/a = 5, 10 and 15%

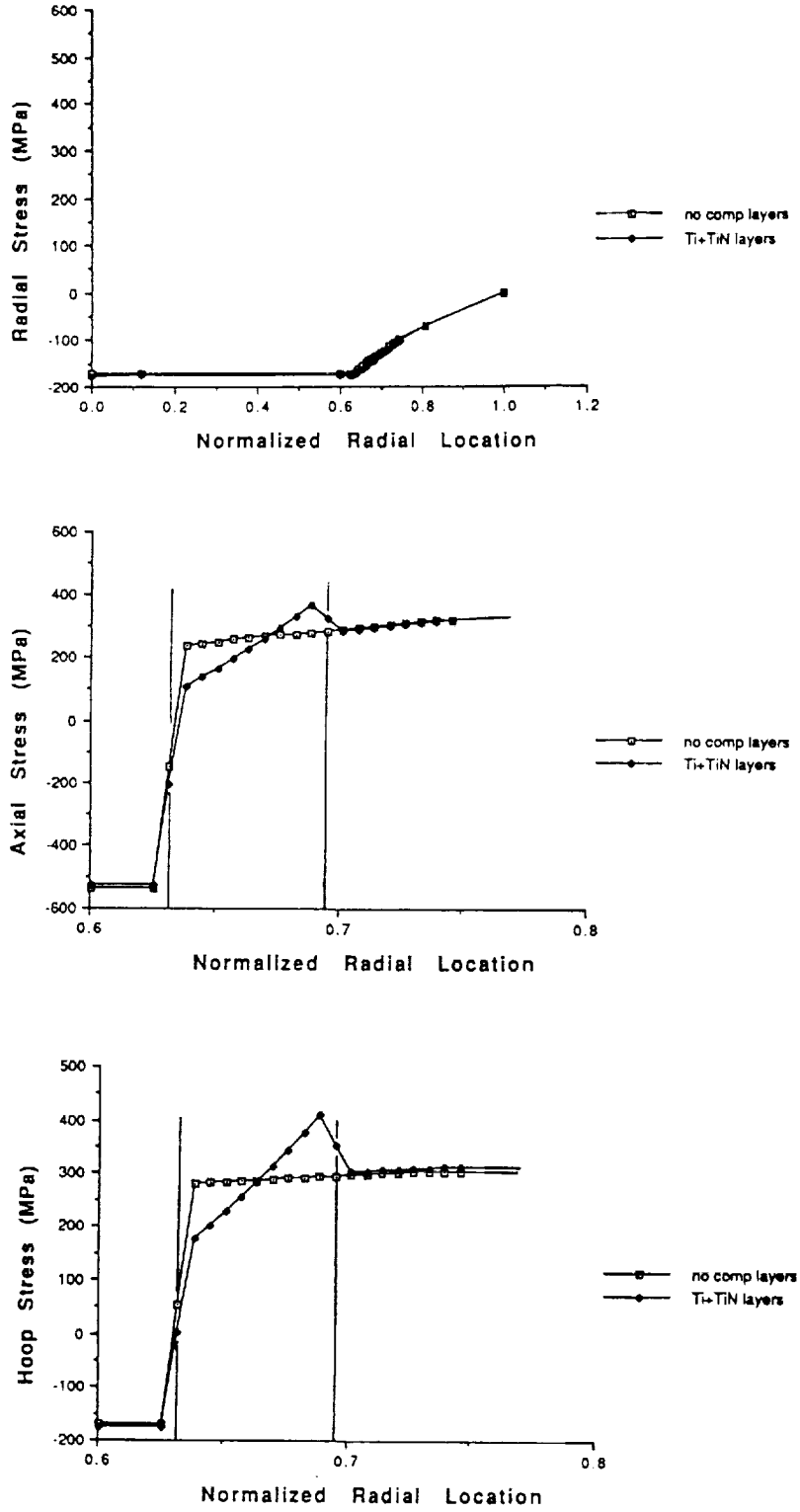

Figure 10. Radial, Axial and Hoop Stresses for SCS-6/Ti_3Al+Nb Showing Effect of a Graded Ti-TiN-Ti Layer t/a = 10%; n = 1

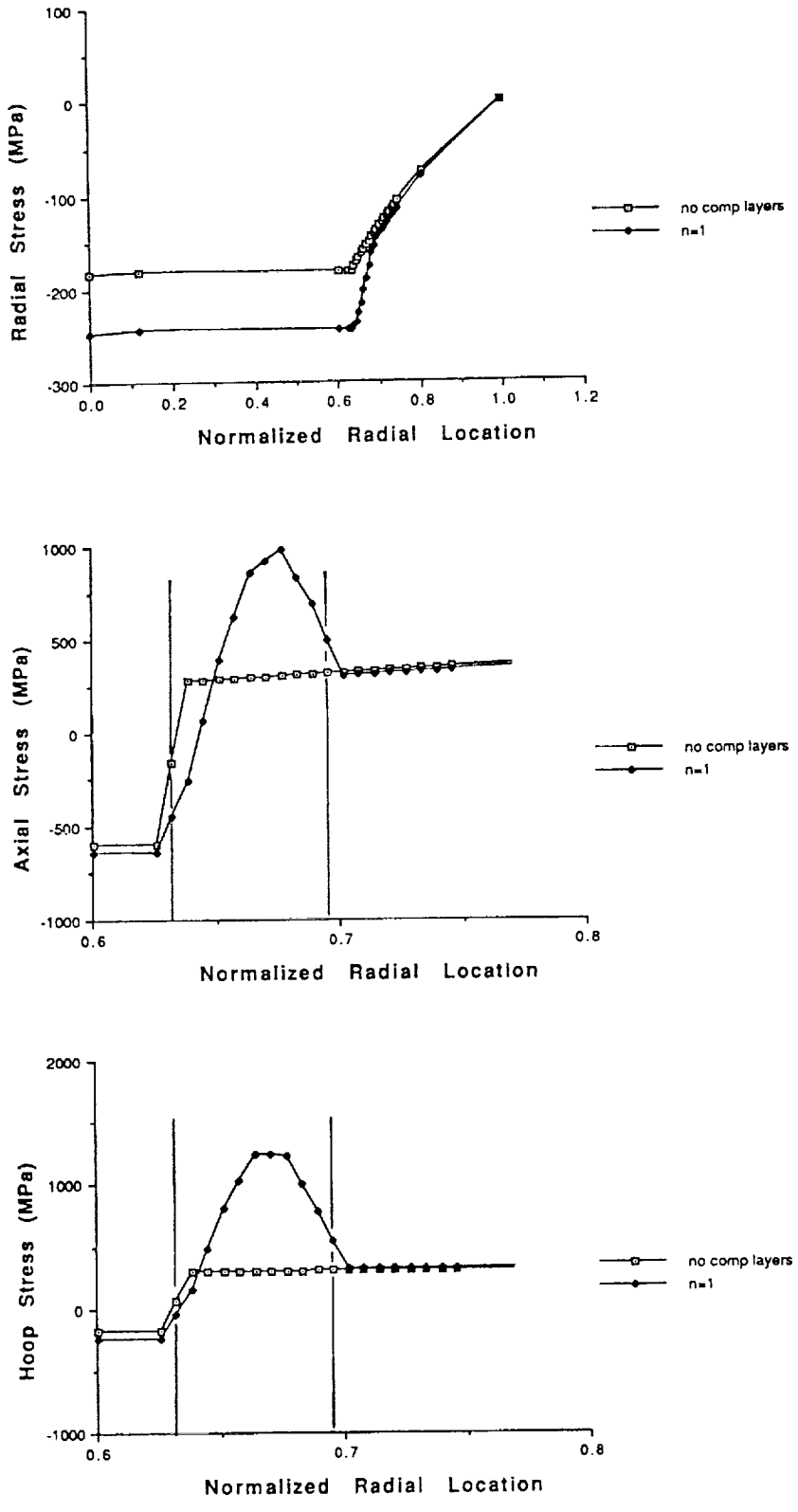

Figure 11. Radial, Axial and Hoop Stresses for Al_2O_3/NiAl Showing Effect of Graded Intermediate Layer t/a = 10%, n = 1

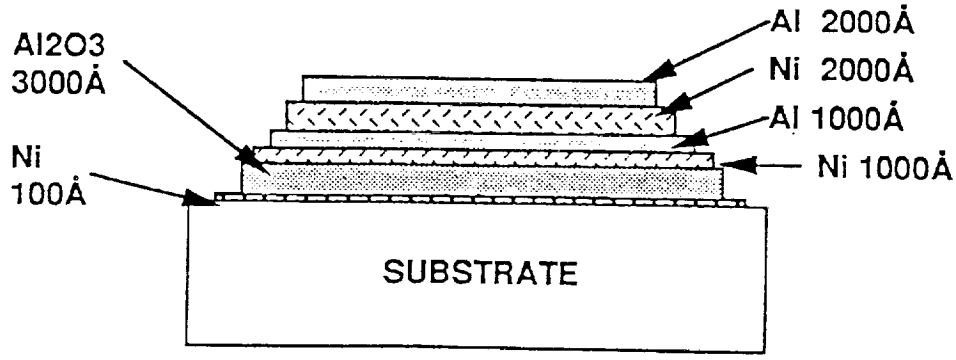

Multi-Layer Design 1

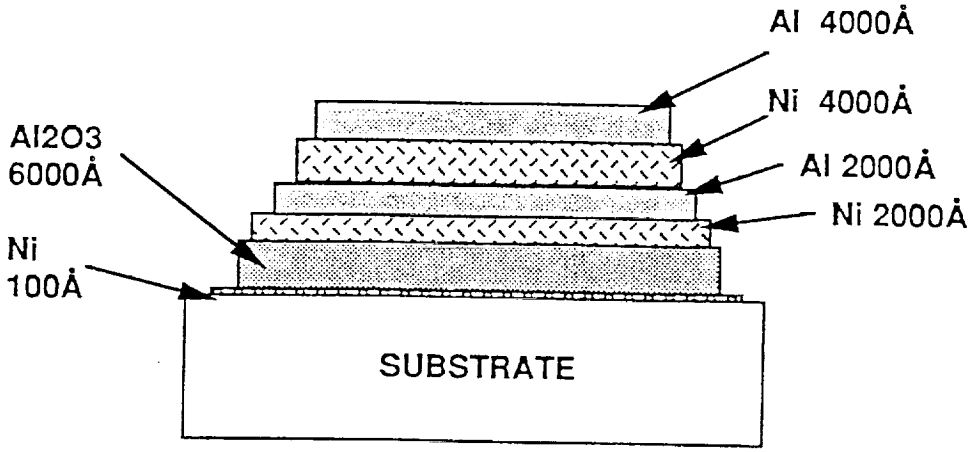

Multi-Layer design 2 - Twice thicknesses of design 1

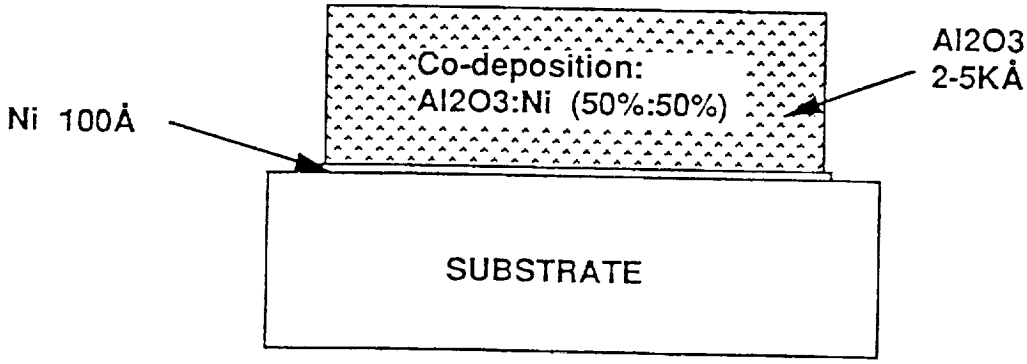

Layer Design 3

Figure 12. Multilayer Designs for Matching CTE Sapphire Substrate and NiAl

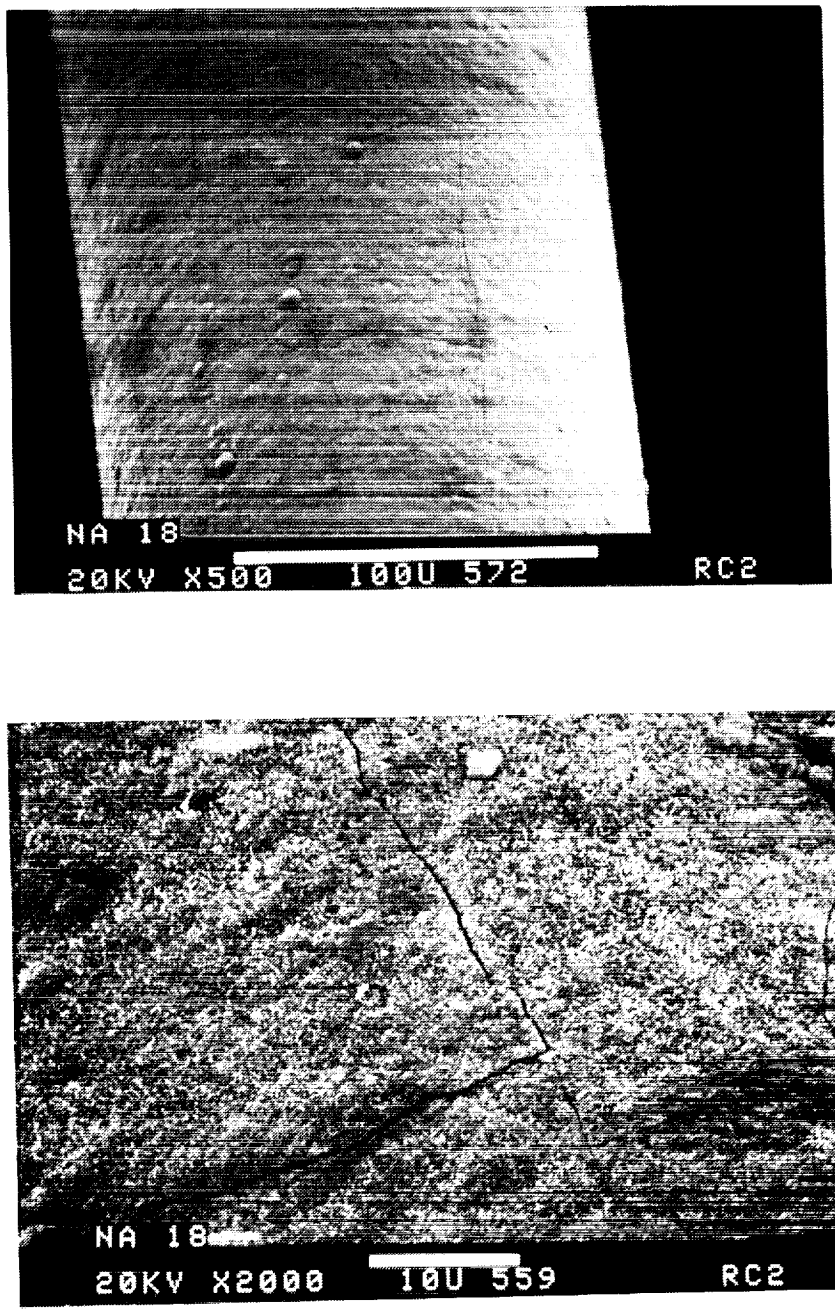

Figure 13. Ti_3Al+Nb Matrix Layer (4.5 μm) on SCS-6 Fiber after Heating at 1050°C for 30 minutes in Vacuum (NA-18)

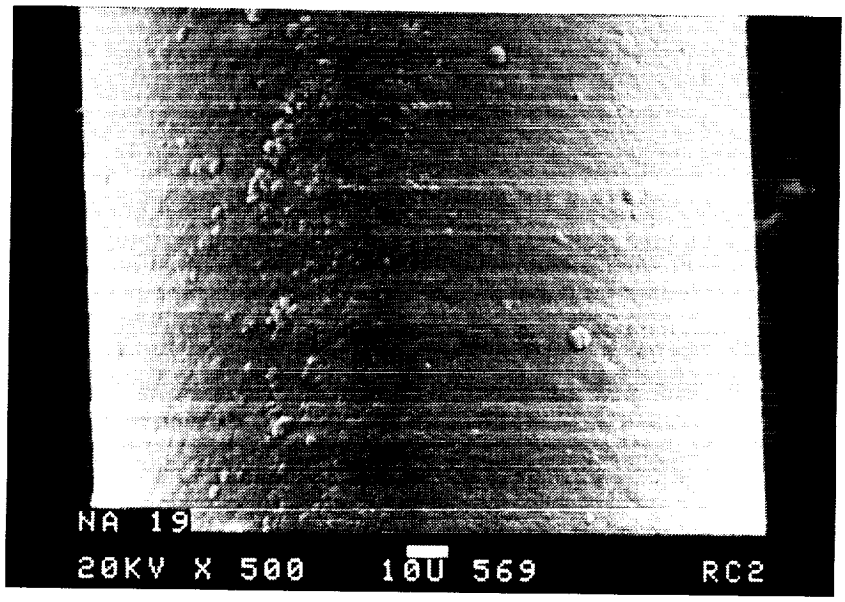

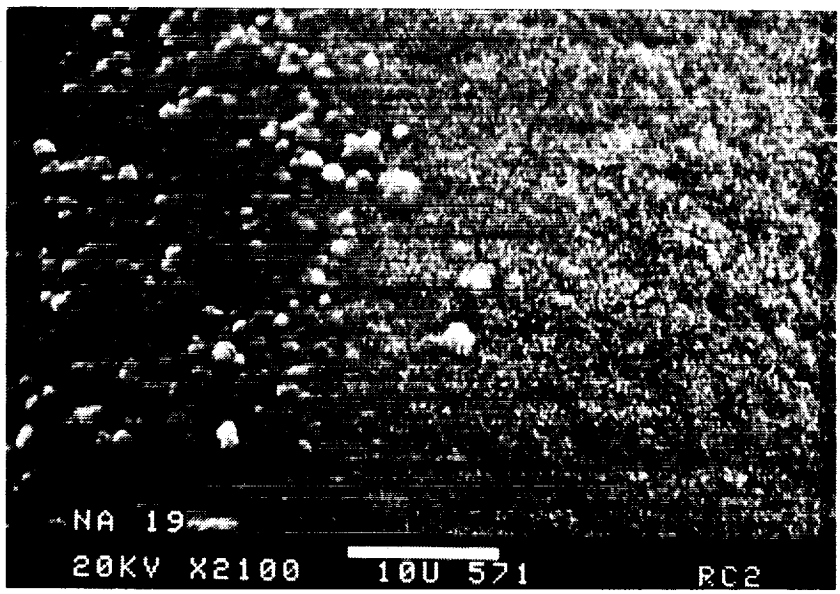

Figure 14. Ti-TiN-Ti (4.5 μm) Graded Layer on SCS-6 Fiber after Heating at 1050°C for 30 minutes in Vacuum (NA-19)

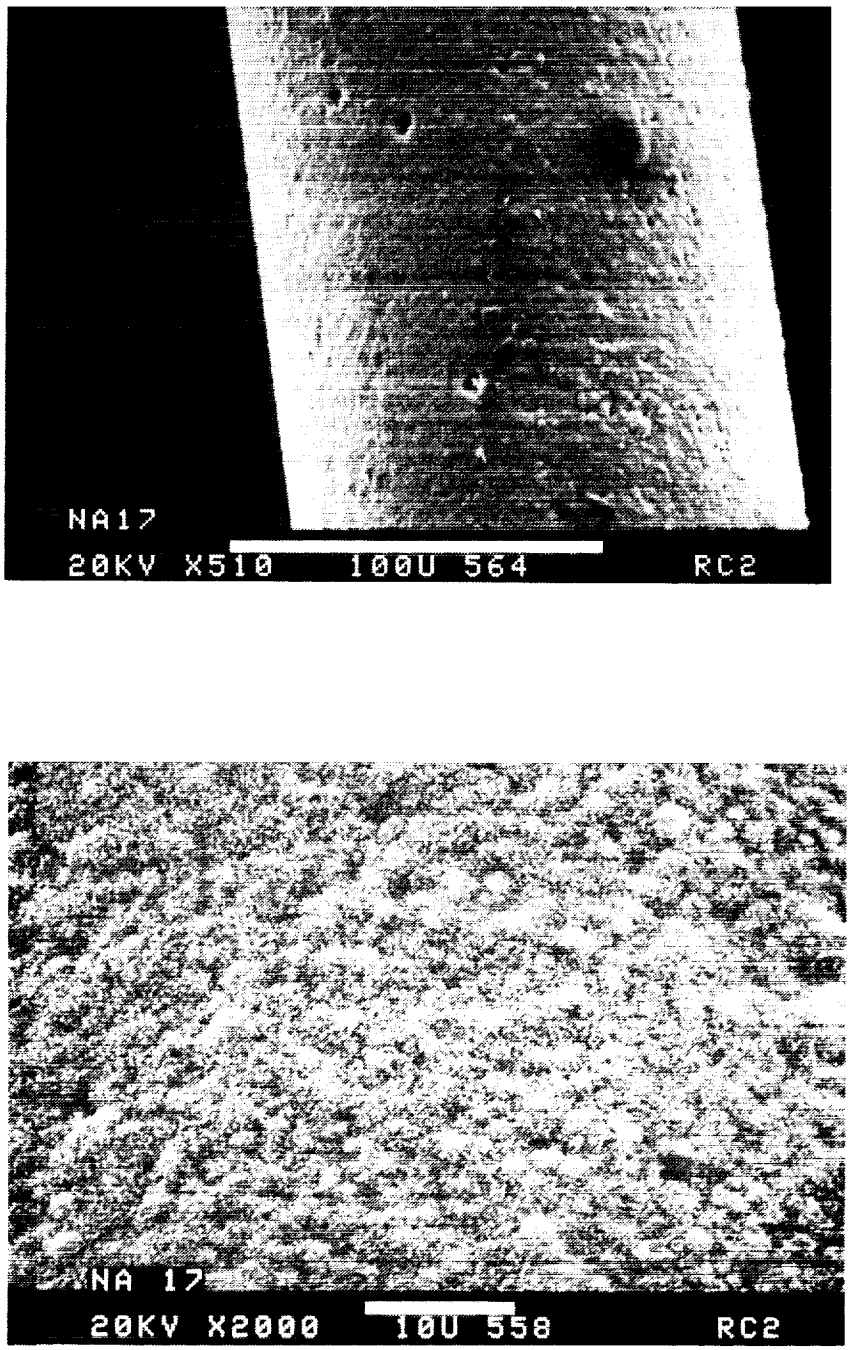

Figure 15. Ti-TiN-Ti (4.5 μm) Graded Layer and 4.5 μm Ti_3Al+Nb Layer on SCS-6 Fiber after Heating at 1050°C for 30 minutes in vacuum (NA-17)

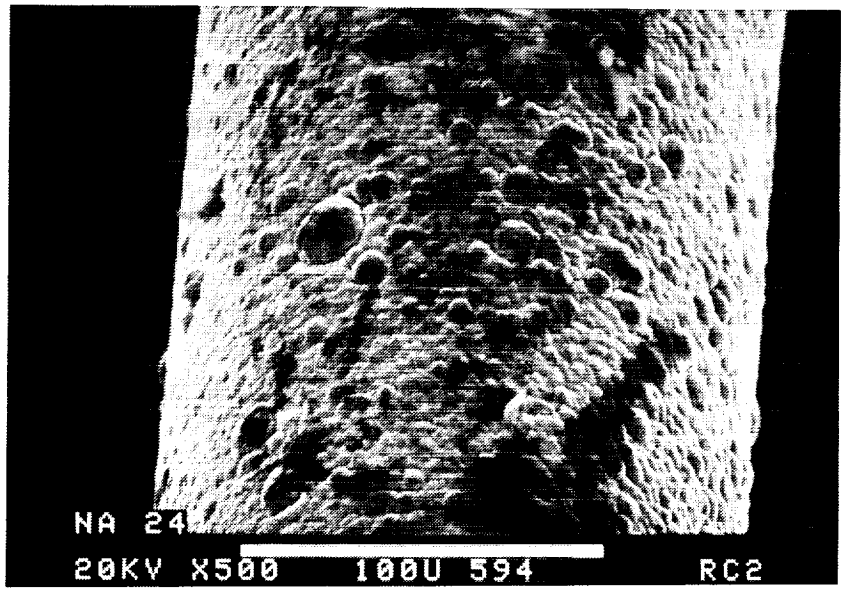

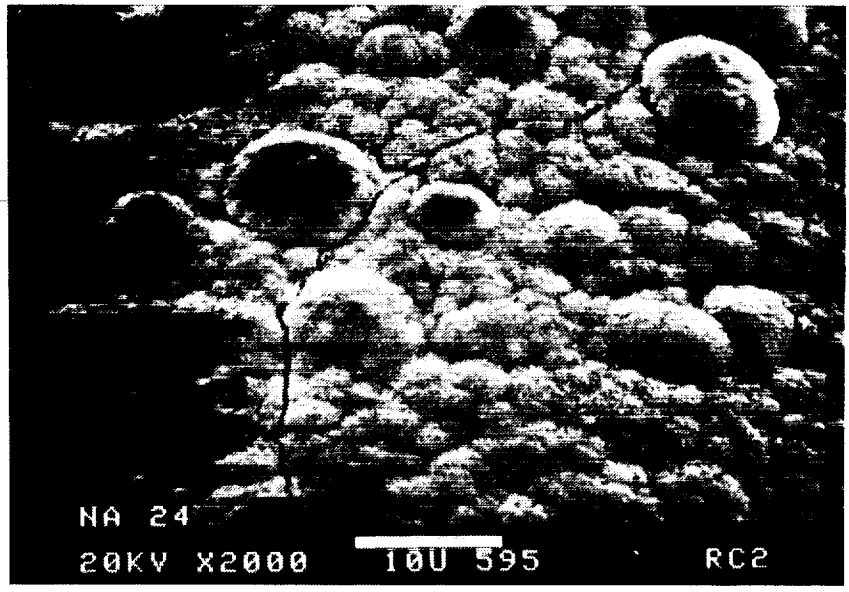

Figure 16. Ti-TiN-Ti (14.5 μm) Graded Layer and 4.5 μm Ti_3Al+Nb Layer on SCS-6 Fiber after Heating at 1050°C for 30 minutes in Vacuum (NA-24)

Figure 17. Cross-Section Appearance of Ni-Al_2O_3-NiAl Graded Layer Before and After Thermal Exposure

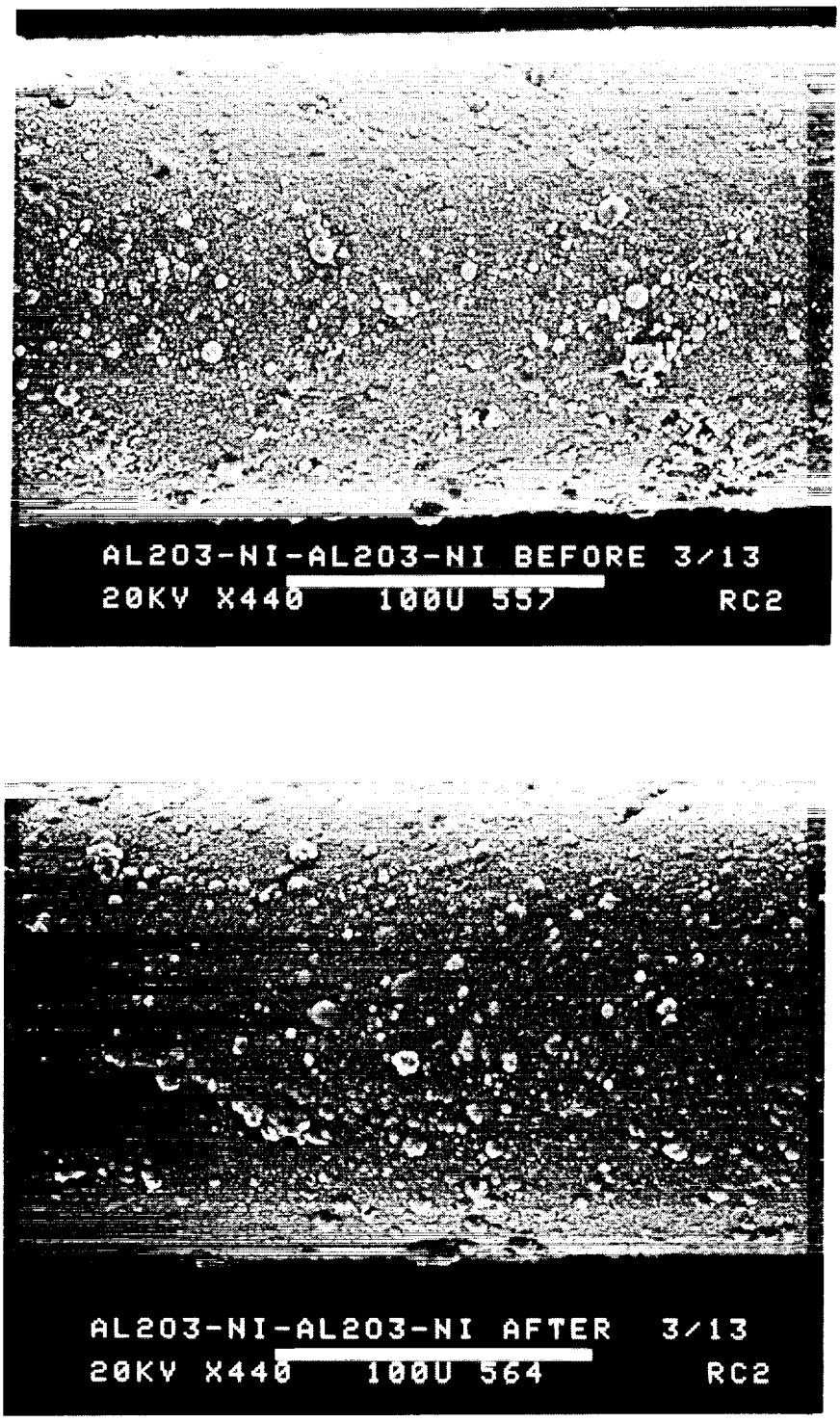

Figure 18. Surface Appearance of Ni-Al_2O_3-NiAl Graded Layer on Sapphire Fiber Before and After Thermal Exposure

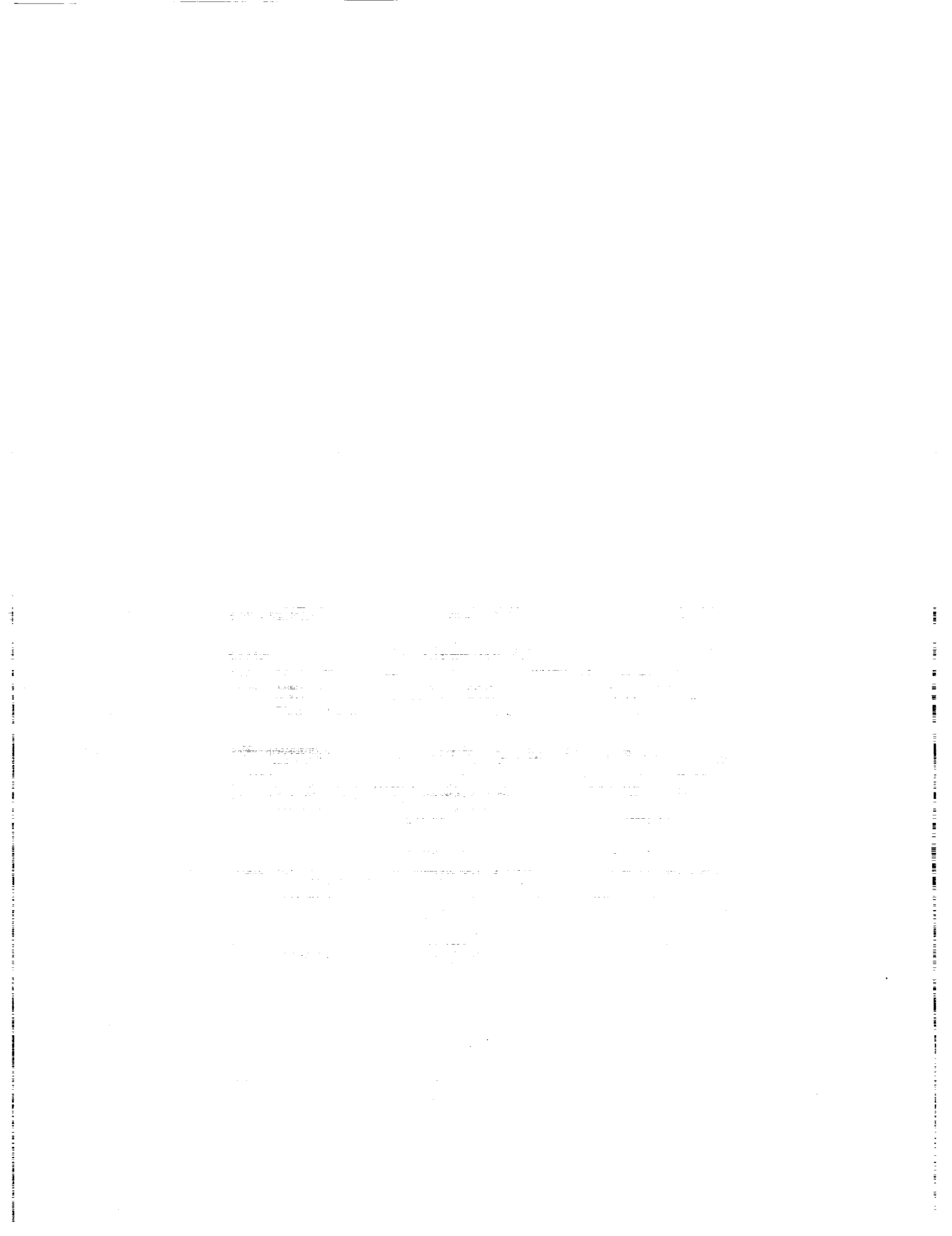

REPORT DOCUMENTATION PAGE

Form Approved
OMB No. 0704-0188

1. AGENCY USE ONLY (*Leave blank*)	2. REPORT DATE	3. REPORT TYPE AND DATES COVERED
	March 1993	Contractor Report

4. TITLE AND SUBTITLE

Advanced Reinforcement Systems for Intermetallic Applications

5. FUNDING NUMBERS

C NAS3-25970
WU 510-01-50

6. AUTHOR(S)

Howard F. Merrick and Mohammed L. Labib

7. PERFORMING ORGANIZATION NAME(S) AND ADDRESS(ES)

Textron Lycoming
550 Main Street
Stratford, CT 06497-7593

8. PERFORMING ORGANIZATION REPORT NUMBER

E-7557

9. SPONSORING/MONITORING AGENCY NAMES(S) AND ADDRESS(ES)

National Aeronautics and Space Administration
Lewis Research Center
Cleveland, Ohio 44135-3191

10. SPONSORING/MONITORING AGENCY REPORT NUMBER

NASA CR-4488

11. SUPPLEMENTARY NOTES

Project manager, Timothy P. Gabb, Materials Division, NASA Lewis Research Center, (216) 433-3272.

12a. DISTRIBUTION/AVAILABILITY STATEMENT

Unclassified - Unlimited
Subject Category 24, 26

12b. DISTRIBUTION CODE

13. ABSTRACT (*Maximum 200 words*)

A 2-D axisymmetric model was employed to determine the magnitude of the radial, axial and hoop stresses caused by the thermal expansion difference between fiber and matrix and which result from the fabrication temperature cycle. Finite element analysis was conducted for single fiber model systems based on SCS-6/Ti_3Al+Nb and Al_2O_3/NiAl. The stress distribution due to the imposition of a graded intermediate layer for each system was determined and included variables of layer thickness and gradation in interlayer chemistry in order to vary the expansion gradient between fiber and matrix. Thermal cycling tests were conducted on sputter coated SCS-6 fibers selectively coated with Ti_3Al+Nb with and without an intermediate layer. Cracking of the Ti_3Al+Nb layers was prevented by an interlayer based on Ti-TiN-Ti. The interlayer thickness appeared critical to its efficiency. Similarly, for the case of Al_2O_3/NiAl, an intermediate layer consisting of a Ni bond coat on the sapphire fiber followed by a graded Al_2O_3-NiAl layer did not crack when given a thermal excursion to 1100 °C and then cooled to room temperature. Acoustic emission tests on single fiber specimens were unsuccessful in detecting load drops associated with the successive fracture of the fiber. For the SCS-6/Ti_3Al system this was the result of several factors which included the matrix/fiber ratio and poor bonding of the matrix and fiber. In the case of the Al_2O_3/NiAl system brittle failure of the NiAl matrix precluded fiber breakdown during tensile loading.

14. SUBJECT TERMS	15. NUMBER OF PAGES
Composite; Intermetallic; Thermal expansion; Functional gradient; Acoustic emission	56
	16. PRICE CODE: A04

17. SECURITY CLASSIFICATION OF REPORT	18. SECURITY CLASSIFICATION OF THIS PAGE	19. SECURITY CLASSIFICATION OF ABSTRACT	20. LIMITATION OF ABSTRACT
Unclassified	Unclassified	Unclassified	

NSN 7540-01-280-5500

Standard Form 298 (Rev. 2-89)
Prescribed by ANSI Std. Z39-18
298-102

NASA-Langley, 1993